Annex F Aerodynamic Impact Assessment

CONTRACT NUMBER: EASA.2020.C02
CONTRACTOR / AUTHOR: DART Aerospace
IPR OWNER: European Union Aviation Safety Agency
DISTRIBUTION: Public

APPROVED BY:	AUTHOR	REVIEWER	MANAGING DEPARTMENT
M.L. Scatola	L. Casciola, M. Eijkman	K. de Cock, M. Selier	DART Engineering

DATE: 26 February 2024

CONTENTS

ABBREVIATIONS

ACRONYM	DESCRIPTION
AOA	Angle of Attack
AOS	Angle of Sideslip
BL	Butt Line
CAD	Computer Aided Design
CAS	Calibrated Air Speed
CFD	Computational Fluid Dynamics
CG	Center of Gravity
CS	Certification Specifications
CP	Static Pressure Coefficient
EASA	European Union Aviation Safety Agency
EFS	Emergency Flotation System
EMS	Emergency Medical Services
ETSO	European Technical Standard Order
FHA	Functional Hazard Assessment
FMEA	Failure Mode & Effect Analysis
FMECA	Failure Mode, Effect & Criticality Analysis
FOM	Figure of Merit
FPM	Feet Per Minute
GPL	General Public License
HEFS	High mounted Emergency Flotation System
HOGE	Hover Out of Ground Effect
IAS	Indicated Air Speed
IFR	Instrument Flight Rules
ISA	International Standard Atmosphere
LH	Left Hand
MCP	Maximum continuous power
MGB	Manual Gearbox
MR	Main Rotor
MTBF	Mean Time Between Failure
MTOW	Maximum Take Off Weight
NPA	Notice of Proposed Amendment
OEI	One Engine Inoperative
PAX	Passengers
PSSA	Preliminary System Safety Analysis
RANS	Reynolds Averaged Navier Stokes
RH	Right Hand
SAR	Search And Rescue
SAS	Stability Augmentation System

SSL	Standard Sea Level
SST	Shear Stress Transport
TOSS	Take Off Safety Speed
TPP	Rotor Tip Path Plane
V_D	Maximum Speed in Dive
V_H	Maximum speed in level flight at MCP
V_{NE}	Speed to never exceed
V_Y	Speed best rate of climb
V_{TOSS}	Take Off Safety Speed

VARIABLES

ACRONYM	DESCRIPTION
α_{TPP}	Angle of attack of the Main Rotor Tip Path Plane
$\Delta Blockage_{MR\|HEFS}$	Variation of Main Rotor Blockage Factor after the installation of the HEFS pods
$\Delta\eta_{TR\|HEFS}$	Variation of Tail Rotor Efficiency after the installation of the HEFS pods
σ	Main Rotor Solidity Ratio
ρ	Generic air density
ρ_{SSL}	Air density at the standard sea level (1.225kg/m^3)
μ	Advance Ratio
ζ	Generic Oscillation Damping factor
θ_0	Collective input on the main rotor blades, measured at 75% of the blade span
γ	Air heat capacity ratio
ω	Generic Oscillation Pulsation
λ_{TPP}	Inflow Ratio
A	Generic rotor disc area
$A_{\|MR}$	Main Rotor disc area
$A_{\|TR}$	Tail Rotor disc area
a_1	Backward flap angle of the main rotor
a_{1s}	Total backward flap angle of the main rotor due to the sum of -B_{1s} and a_1
B_{1s}	Longitudinal cyclic pitch angle of the swash plate, positive is forward tilt (nose down response)
CAS_{CFD}	Calibrated Airspeed obtained from CFD simulation
Cd	Generic Drag Coefficient
C_{D0}	Drag Coefficient related to the front surface of the helicopter fuselage
Cl_α	Generic Lift Coefficient Derivative to Angle of Attack
$D_{fuselage+tail+mast}$	Drag of Helicopter Fuselage, Tail and Main Rotor Mast
g	Gravitational acceleration
H_{MR}	Drag Force of the Main Rotor
H_{TR}	Drag Force of the Tail Rotor
HP	Pressure Altitude
IAS	Generic Indicated Airspeed
$IAS_{baseline\ helicopter}$	Indicated Airspeed measured in the baseline helicopter
k	Main Rotor blade twist in radians
K_{HP}	Correction coefficient for the Pressure Altitude
K_{IAS}	Correction coefficient for the Indicated Airspeed
L	Characteristic length of the blunt body
m	Helicopter Mass
M_α	Pitch Moment derivative induced by a change in Angle of Attack
M_a	Generic Moment derivative with respect to a generic parameter
M_q	Pitch Moment derivative induced by a change in Pitch Angular Speed
M_u	Pitch Moment derivative induced by a change in variations in flight speed

N_v	Yaw Moment derivative induced by a change in sideslip angles
N_R	Yaw Moment derivative induced by a change in Yaw Angular Speed
$P_{i\|MR}$	Main Rotor Induced Power
$P_{i\|MR,HEFS}$	Main Rotor Induced Power after the installation of the HEFS pods
$P_{i\|TR}$	Tail Rotor Induced Power
$P_{i\|TR,HEFS}$	Tail Rotor Induced Power after the installation of the HEFS pods
$P_{profile+Hforce\|MR}$	Power dissipated for drag forces in the Main Rotor
$P_{profile+Hforce\|TR}$	Power dissipated for drag forces in the Tail Rotor
P_{static}	Static Pressure
P_{total}	Total Pressure
P_{SSL}	Static Pressure at Standard Sea Level (101325 Pa)
S	Frontal area of the helicopter fuselage
St	Strouhal Number
T_{MR}	Main Rotor Thrust
$T_{MR\|x}$	Forward component of Main Rotor Thrust
T_{TR}	Tail Rotor Thrust
u	Induced airspeed through the actuator disc surface
u_{MR}	Induced airspeed through the Main Rotor actuator disc surface
u_{TR}	Induced airspeed through the Tail Rotor actuator disc surface
V	Generic Aircraft True Speed
V_0	Aircraft True Speed at a given flight condition
V_{tip}	Relative wind speed experienced by the rotor blades' tip
$V_{tip\|TR}$	Relative wind speed experienced by the Tail Rotor blades' tip
$V_{tip\|MR}$	Relative wind speed experienced by the Main Rotor blades' tip
X_u	Forward acceleration induced by a variations in flight speed
Y_V	Lateral acceleration induced by a change in Lateral Speed
Y_R	Lateral acceleration induced by a Yaw Angular Speed
Z_α	Vertical acceleration induced by a change in Angle of Attack
Z_u	Vertical acceleration induced by a variations in flight speed

1. Approach Aerodynamic Impact Assessment

1.1 Assessed Aerodynamic Effects

The aerodynamic evaluation has established the aerodynamic impact of the HEFS installation in relation to performance and handling qualities (stability and control) requirements. When aligning the task scope with EASA, the agency has referenced specific CS29 and CS27 articles as outlined below.

1.1.1 Handling Qualities

The effect on the static longitudinal stability in cruise has been evaluated in accordance with CS29 Appendix B *IV*(c). Three speeds were assessed: 80 kts, 110 kts and 140 kts. The CS27 related article (CS27 Appendix B *IV* (b2)) is the same as for the CS29.

1.1.2 Performance

The OEI climb performance has been evaluated in accordance with CS29.67 (CS29.67(a)(1)(iii)) and Vy (CS29.67(a)(2)(iii)). Three speeds were assessed: 80 kts, 110 kts and 140 kt. This has indicated wether the installation could jeopardize the Category A performance. For evaluation of the CS27 rotorcraft, the equivalent IFR Category A CS 27 requirements are applicable, which refer to CS29 articles.

1.2 Additionally Assessed Aerodynamic Effects

The HEFS pods can lead to increased drag and alteration of flow around the fuselage which can affect the aerodynamic forces and moments of the helicopter. Potentially, the helicopter performance and handling qualities can be affected, which is captured in the regulatory context presented in the previous section. The installation of a pod in the vicinity of the main rotor and engine inlet could potentially also lead to undesired phenomena listed below. In the assessment of the aerodynamic impact of the pods, these effects have been considered in addition to the performance and handling qualities mentioned above.

- Changes in aerodynamics forces and moments which can lead to a change in static margins of the helicopter commands.
- Higher drag force and power consumption, which leads to an increase in the required engine power both in hover and in forward flight.
- Creation of shed vortices from the pod, which could lead to additional vibrations in the structure.
- Flow disturbances at engine inlet, depending on the location of the HEFS pod in relation to the engine inlet. In case the pod is located near or upstream of the engine inlet, the air flow quality entering the engine may be disturbed to a level that impacts engine performance.

1.3 Flight Conditions

The helicopter mission profile can be approximated by a finite number of points in the flight envelope. Each point represents a stable flight condition at which it is possible to evaluate the aircraft performance (equilibrium conditions), static stability, and qualitative airflow characteristics. The aim of the analysis is to evaluate the impact of the newly installed pods with respect to the default helicopter configuration with lower flotation systems installed. It was decided to analyze both the CS29 and CS27 helicopter at the flight conditions as presented in Table 1, since the CFD model was extensively validated for these speeds with available data for validation.

Flight condition	Simulated Conditions	Remarks
200 ft AGL, climb	75kts with AOA reduced by 5deg and rotor thrust increased 1.1 times, landing gear drag added in post analysis	OEI steady climb rate impact, extended landing gears
Cruise	80kts, level	Longitudinal stability Lateral stability
Cruise	110kts, level	Longitudinal stability Lateral stability
Cruise	140kts, level	Longitudinal stability Lateral stability

Table 1 Flight conditions analysed

To compute the Aerodynamic Derivatives, simulations are repeated varying one parameter at the time according to Table 2.

Derivative	Condition Change	Remarks
$\partial \boldsymbol{u}$	$\pm 5kts$ CAS	Two additional Simulations -Helicopter in the same attitude -Same Rotors parameters -Same Engine parameters
$\partial \boldsymbol{v}$	$\pm 5kts$ CAS	Two additional Simulations -Helicopter in the same attitude -Same Rotors parameters -Same Engine parameters
$\partial \boldsymbol{w}$	$\pm 5kts$ CAS	-Two additional Simulations -Helicopter with different AOA -Same AOS -Same Rotors parameters -Same Engine parameters
$\partial \boldsymbol{p}$	$\pm 12deg/sec$ along x-axis	-Two additional Simulations -Multiple Reference Frame to simulate instantaneous rotation -Helicopter in the same attitude -Same Rotors parameters -Same Engine parameters
$\partial \boldsymbol{q}$	$\pm 12deg/sec$ along y-axis	-Two additional Simulations --Multiple Reference Frame to simulate instantaneous rotation -Helicopter in the same attitude -Same Rotors parameters -Same Engine parameters
$\partial \boldsymbol{r}$	$\pm 12deg/sec$ along z-axis	-Two additional Simulations --Multiple Reference Frame to simulate instantaneous rotation -Helicopter in the same attitude -Same Rotors parameters

		-Same Engine parameters

Table 2 Derivative calculations

As described above, to limit the aerodynamic assessment scope it is necessary to identify an average helicopter mission profile for relevant representative configurations of helicopters in the European offshore fleet and requiring ditching certification in accordance with the Air Ops Rules. Depending on the helicopter configuration and mission, some of aerodynamic effects of the HEFS pods might be more limiting than others Therefore, a selection of relevant flight conditions is made for each of the aerodynamic effects analysed in the aerodynamic impact assessment.

1.4 Top-level approach and Rationale

In the scope of this study, CFD is the chosen method to assess the aerodynamic impact of the HEFS. Despite the fact that the number of simulations is quite high, the complete freedom of design iteration and the lower execution costs have driven the choice toward this solution. The top-level approach is visualised in Figure 1. These choices are a trade-off on availability of resources (time, effort, hardware and software), availability of data, and the required accuracy for the results in view of the project objectives. In summary, the approach entails the steps described below.

- CAD modelling of the baseline helicopter and the helicopter with HEFS pods installed
- Development, validation and execution of the CFD framework in three phases :
    - **Phase 1**: Set-up and validation of the CFD analysis using data provided by the TC HOLDER. Key in successful validation is that the accuracy of the models should be sufficient to capture the 'impact', being the 'delta' between the baseline helicopter and the HEFS equipped helicopter. Absolute accuracy is not required but beneficial, since this is not a certification project.
    - **Phase 2**: Exploration and verification of set-up accuracy (e.g. meshing quality, boundary conditions) versus simulation time to achieve an optimum between accuracy and computational performance.
    - **Phase 3**: Generation of data and results.
- Handbook Methods analysis, using the CFD data to evaluate the aerodynamic impact in terms of performance and handling qualities, and assessment if this impact is 'acceptable'. This is done firstly in CFD phase 2 to get first impressions and test the methods, and finally with the resulting data from CFD Phase 3.

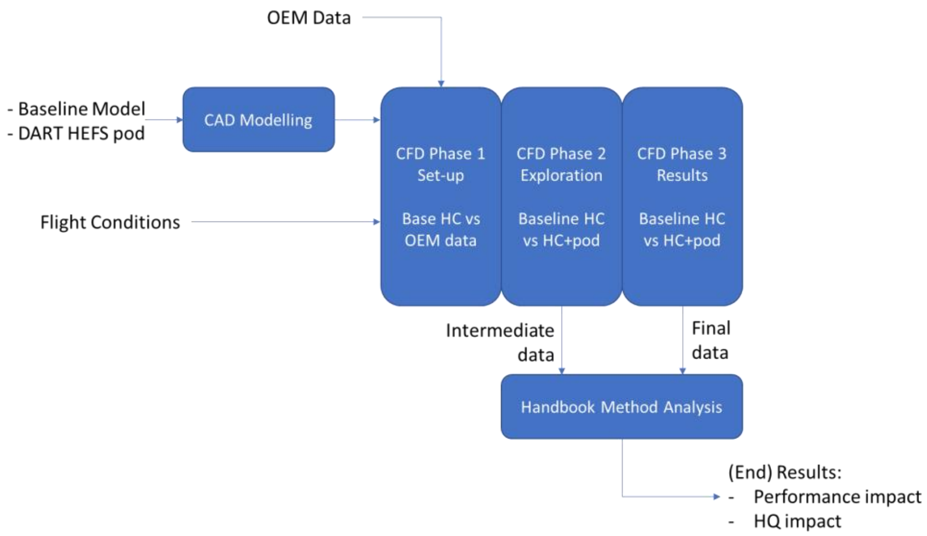

Figure 1 Top-level approach for HEFS Aerodynamic Impact Analysis

1.5 Computational Fluid Dynamics Analysis

In the scope of this study, CFD software has been used to assess the aerodynamic impact of the HEFS. The software that has been used to perform CFD simulations is OpenFOAM (Open Field Operation And Manipulation), a GPL C++ toolbox based on continuous mechanics that includes CFD. The image below presents an overview of the software available to work with OpenFOAM that was selected for the scope of this project. OpenFOAM has proved to provide reliable results in aerospace in various studies such as in (Antoniadis, et al., 2012), (M. Fuchs, F. Le Chuiton, C. Mockett, J. Sesterhenn and F. Thiele, 2015) and (Mockett, 2012).

GEOMETRY	MESHING	SOLVER	AUTOMATION	POSTPROCESSING
Solidworks	CfMesh	openFOAM	Python	Python
				Paraview

OpenFOAM | Open Source Third Party | Commercial Package

Figure 2 OpenFOAM framework

The aim of the CFD-analysis is to capture the aerodynamic effects introduced by the pods with respect to the helicopter's baseline aerodynamic design, as certified by the manufacturer. The quality and the detail of the analysis has been adapted and evaluated with respect to the simulation time, depending also on the hardware available, and the specific phenomena that must be quantified. To obtain access to the required level of hardware, a cloud computing virtual machine system has been deployed that matches the required standards in terms of computing power, cybersecurity and storage. Aerodynamic CFD data has been extracted and analyzed using data analysis tools written in Python programming language. Routines were implemented to automatically compare the results and to generate various plots and images. The meshing process was carried out with the commercial package CfMesh and the CAD model originates from Solidworks.

1.5.1 Validation Approach of the CFD Model

For this study, the CFD model has been validated by a combination of expert engineering judgement and comparison to TC HOLDER furnished data, as far as available. For the scope of this project, the CFD should be capable of determining the 'delta impact' from adding the HEFS, and capture flow phenomena expected from adding the HEFS in the prescribed location.

Expert engineering judgement is applied throughout the entire process with the aerodynamic engineers making choices in modelling (e.g. numerical set-up) and senior experts reviewing and challenging. Also, the results have been (peer) reviewed against expectation.

The TC HOLDER has provided the following validation information and images for the baseline CS29 reference helicopter which excluded the Hoist and the Landing Gear:

- Distribution of the Pressure Coefficient C_p over the fuselage in one generic forward flight condition: this information is provided in the form of images which are the results of a CFD simulation. The TC HOLDER also provided information about the simulation settings and helicopter attitude.
- Helicopter Drag at various CAS and at SSL (ISA)

The CFD pressure coefficient distribution data has been compared with the CFD pressure coefficient distribution data computed in this study. To assess similarities and differences that have been found, guidelines were sought in a state-of-the-art comparison of helicopter aerodynamic results obtained by different CFD codes as reported in (Antoniadis, et al., 2012). The computed helicopter drag data at various CAS and at SSL (ISA) provided by the TC HOLDER has been compared with the CFD drag data computed in this study.

The TC HOLDER has provided the following information and images for the baseline CS27 reference helicopter:

- Power required vs. calibrated air speed, TOW 2500 Kg, 1000ft, ISA+20 (without additional information this cannot be used for validation as it would require too many rough estimations).
- Centre of Gravity Diagram

1.5.2 Data Extracted from CFD Simulations

To provide a full picture of the aerodynamic changes after the installation of the HEFS, the CFD simulations included measurement points, computation of forces and cross-sectional planes that have been used to compute the aerodynamic quantities.

Specifically, the following information has been yielded:

- *Aerodynamic forces and moments*: Pressure data and shear stresses were integrated over the helicopter body to obtain forces and moments around the CG. The forces were then projected into the main flow components to find the delta in Fuselage Drag and Fuselage Down-Lift.
- *Increased wake cross-sectional area*: a series of planes have been placed in the helicopter wake propagation area to evaluate the effect of the pods on the flow downstream of the helicopter fuselage.
- *Creation of shed vortices originating from the pod*: in both high and low speed conditions the shedding frequency of vortices from the pods was investigated. By using the Strouhal number which is related to the local Reynolds number and the shape of the pod, the frequency of shed vortices can be determined.
- *Flow disturbances at engine inlet*: the engine inlet has been approximated as a mass flow outlet (flow out of the computational domain). The flow at the inlet has been evaluated for the CS29 as this inlet is placed directly downstream of the pod. The quality of the flow at the engine inlet has been evaluated in terms of total pressure recovery and total pressure distortion. It was agreed with EASA that this evaluation is not necessary for the CS27, as the engine inlet is placed beneath the pod, where no disturbances induced by the pods are expected.
- *Loss of efficiency in the horizontal tailplane and vertical fin*: A high level analysis has been performed to evaluate the change in flow quality near the tailplane and fin, which could induce a difference in aerodynamic forces.

1.6 Performance and Helicopter Handling Quality

For the evaluation of the helicopter performance and handling quality, three aspects have been investigated within the scope of this project: a static stability analysis and One Engine Inoperative (OEI) climb performance. In this section the approach taken for this assessment is described.

1.6.1 Analysis of Quantitative Aerodynamic Data

Once the aerodynamic data is obtained, it is possible to quantify the helicopter performance and handling quality. For this study, handbook methods have been used to do this, evaluating helicopter performance losses and the degradation in the handling quality.

The helicopter performance analysis is based on three books:

- U.S. Naval Test Pilot School Flight Test Manual: Rotary Wing Performance (U.S. Naval Test Pilot School, 1996)
- A. K. Cooke: Helicopter Test and Evaluation (A. Cooke, E. Fitzpatrick, 2002)
- M. Arra: L'elicottero (Arra, 2001)

The Climb with One Engine Inoperative is one of the critical conditions to be certified, both for the CS29 and the CS27 Category A. The helicopter power system must ensure that one engine working at its Maximum Continuous Power can deliver enough power to climb at a specific speed and at a specific Rate Of Climb. To evaluate this, it is possible to establish the variation in power consumption in climb after the installation of the pod, verifying that the engine can deliver enough power to fly at the given CAS, and to increase the potential energy of the CG at a given rate. The engine data provided by the TC HOLDER only refers to the 30 min OEI power limit, therefore the validation of the ROC requirements will be held against the requirement CS29.67.a.2, and that should be conservative if compared to the requirement CS29.67.a.1. The CFD simulations have been performed in a climb attitude and the baseline helicopter configuration has been also simulated to verify the power margins available in the OEI condition. In these simulations, the exhaust gas has been simulated only exiting from one engine, the one which is less capable to re-energize the helicopter wake (depending on the aircraft attitude).

The static stability of the helicopter has been analysed in consideration of the handling quality of the helicopter. According to regulations, the control stick position should have a positive gradient. In each flight condition, both helicopter configurations have been evaluated in terms of static stability on the longitudinal axis. Given a combination of helicopter configuration and a flight envelope test point, five simulations were performed to obtain the static stability margin. First, a simulation provided the data related to the flight condition flown at a given CAS, then two additional simulations were performed with -5knots CAS and +5knots CAS and with the helicopter maintained at the same attitude, then other two simulations were performed with a pitch rate of +0.2 rad/s and -0.2 rad/s respectively. By comparing the static stability margin associated with the baseline helicopter and the one relative to the helicopter with pods, it is therefore possible to estimate the change in longitudinal static stability.

For both CS29 helicopter and CS27 helicopter, the longitudinal static stability should guarantee sufficient margins of change. For the purpose of this delta study, it is assumed that deltas in static stability margins < 10% are negligible, whereas deltas exceeding 10% indicate an area of attention which should be further validated, for example in flight tests.

1.7 Reference Helicopter Models

A CS29 Reference Helicopter model was created for use in CFD simulations with symmetric engine inlets. The 17 meters long aircraft has a 5 bladed main rotor with a diameter of 13.8 meters and a 6400 kg MTOW (EASA, Type Certificate Data Sheet for AW139, 2021). The rotor Solidity Ratio $\sigma = 0.08$. A CS27 Reference Helicopter model was created for use in CFD simulations that includes symmetric engine inlets and main gear box inlets. The 12 meters long aircraft has a 4 bladed main rotor with a diameter of 10 meters and a 2800 kg MTOW (EASA, Type Certificate Data Sheet for EC135, 2022). The rotor Solidity Ratio can be approximated to $\sigma = 0.1$. The CAD models include information about the diameter and position of the rotors, as well as volumes and constraints that limits the HEFS pod design and installation area. In its final version, the model also includes all the components and NACA inlets that are present in the upper cowling area that are considered when designing the pods. For the reference helicopters, the following parameters are considered using inputs from the aircraft manufacturer:

- Helicopter mass and Inertia
- Helicopter Attitude and Main Rotor Tilt at various CAS (only for CS29)
- Main Rotor Thrust and Torque at various CAS (only for CS29)
- Various Engine parameters (only for CS29)
- Images showing the CP distribution over the helicopter body, no rotors included in the simulation (only for CS29)

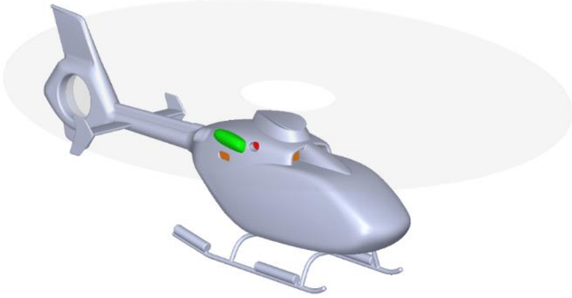

- Drag of the fuselage at various airspeeds (only for CS29)
- Power required vs. calibrated air speed (only for CS27)

Figure 4 CS27 Reference Helicopter CAD model including HEFS pods for CFD simulation

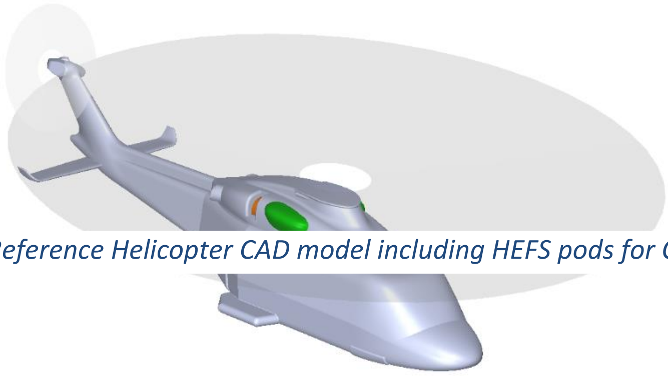

Figure 3 CS29 Reference Helicopter CAD model including HEFS pods for CFD simulation

The CAD models of both the CS27 and CS29 reference helicopters have been entirely processed to meet the required standards for CFD simulations. Parts have been converted to solid bodies using Solidworks® and components with zero-contact faces have been overlapped. Rotors have been converted to 2-dimensional bodies and shapes have been parametrized.

The HEFS pods have been inserted as an aerodynamic shape to be simulated with the rest of the helicopter as shown in Figure 3 and Figure 4. The presence of the High mounted EFS goes along with the presence of the EFS installed in the main fuselage underbelly structure. The volume related to the HEFS cylinder has been positioned according to the buoyancy analysis performed in this project with the float bag oriented parallel to the aircraft X-axis. The pods have been positioned in such a way that they do not obstruct the engine inlet or other inlet vanes and to remain in the area of the upper cowling external surface in the case of the CS29, see Figure 5 showing the CS29 case.

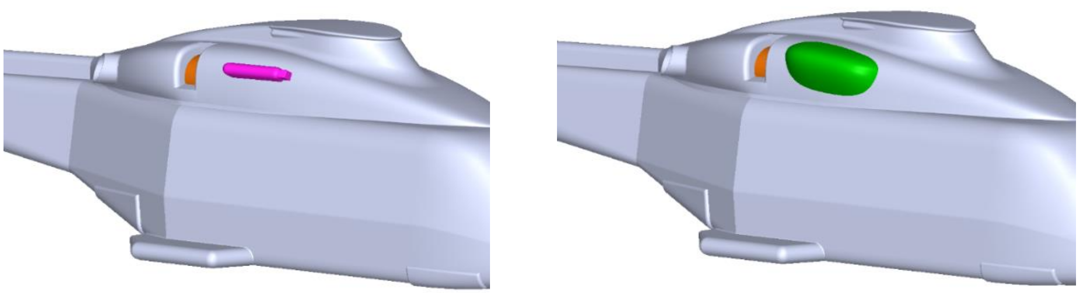

Figure 5 CS29 Reference Helicopter View of HEFS device contained inside pod (left) and of pod (right)

1.8 Engine Simulation in CFD

The CFD simulation does not include a direct simulation of the engine as the complexity of the simulation would increase significantly and the result would become too dependent on (certification of) the specific helicopter type whereas this study aims to cover the CS29 and the CS27 class globally. Therefore, the engine is simulated by setting *mass flow rate* boundary conditions at the engine inlet and engine outlet. At the engine inlets (right of Figure 7 and orange patch in **Error! Reference source not found.**), a mass flow rate boundary condition out

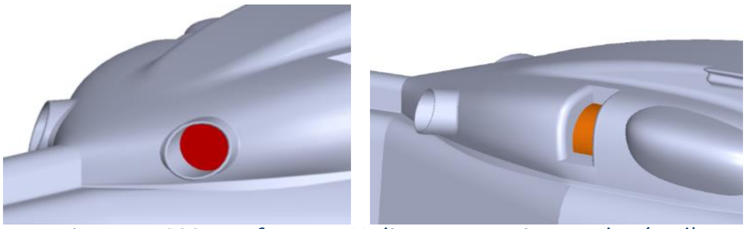

Figure 7 CS27 Reference Helicopter engine outlet (red) and engine inlet (orange)

Figure 6 CS29 Reference Helicopter Engine outlet (left) and engine inlet (right)

of the domain is used and at the engine outlet (left of Figure 7 and red patch in **Error! Reference source not found.**) a mass flow rate into the domain is used. The mass flow into the domain equals the mass flow out of the domain.

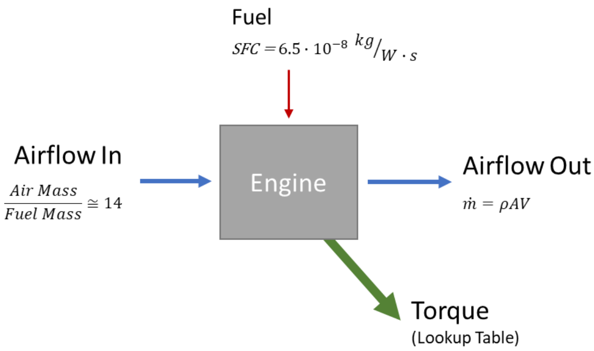

Figure 8 Engine Modelling Scheme for this study

The mass flow of air through the engine inlet and outlet is approximated following the schematic presented in **Error! Reference source not found.**. The following two cases are given as example. From typical engine data for the CS29 reference helicopter, a reference power is selected which is needed to fly at 110 kts. From data related to the CS27 reference helicopter provided by the TC HOLDER, a reference power is selected which is needed to fly at 110 kts. The engines have a Specific Fuel Consumption which provides an estimation of the fuel injected in the combustion chamber. The combustion requires a well-defined air mass to fuel mass ratio to be established, which in this case is set to be a constant of 14. The equation used to obtain the mass flow rate of air at the engine inlet and outlet can be found below.

$$\dot{m} = SFC \cdot P \cdot \frac{Air\ mass}{Fuel\ mass}$$

$$SFC = 6.5 \cdot 10^{-8} \left[\frac{kg}{W \cdot s}\right]$$

Which results in a mass flow of air into and out of the engine for a 110 kts reference speed. Additionally, the CS27 also has inlets and outlets for the main gear box. These can be seen in **Error! Reference source not found.**, where the main gear box inlet is colored in orange at the most forward part of the helicopter, and the main gear box outlet is colored red. The mass flow through the main gear box inlet and outlet is assumed to be equal to the freestream mass flow at the particular flight speed at which the simulation is modelled, according to the following formula:

$$\dot{m}_{gearbox} = (1-B)\,\rho\,V\,A_{gearbox-inlet}$$

Where B constitutes the blockage factor of the cooling system which is 0.4 for a passive ducted radiator.

1.8.1 Analysis of Engine Inlet Flow Quality

For the CS29 reference helicopter, it is relevant to assess the quality of the flow ingested by the engine. For this assessment, the total pressure is evaluated in a plane near the engine inlet. In this study, the flow quality ingested by the engine was analysed by looking at the following characteristics of the flow near the engine inlet:

- Total pressure recovery with respect to the freestream total pressure
- Distortion of total pressure distribution (asymmetry in x- and y-direction, outliers)

For the CS27 reference helicopter, the engine inlet is located below the HEFS pod. Since the engine inlet is not directly downstream of the pod as was the case for the CS29 reference helicopter, no critical changes imposed by the pod on the quality of the flow ingested by the engine are expected.

1.9 Computational Fluid Dynamics Framework

1.9.1 Rotor Disc Simulation and Moving Reference Frame

To simulate a rotor disc in a CFD Finite Volume solver, the following three possibilities were considered: Unsteady Simulations, Steady Simulations with Moving Reference Frame, and Steady Simulations using an Actuator Disc. In this study a Constant Inflow Actuation Disc model was used for both the main rotor and the tail rotor. The constant inflow actuation disk model was implemented into the OpenFOAM framework and the validation of the model was carried out by comparing the downwash profile and magnitude on the disk longitudinal section plane. To derive the aerodynamic derivatives with respect to p, q and r, it is necessary to simulate the instantaneous act of rotation of the helicopter. To do so, a moving reference frame is implemented in the OpenFOAM framework used. The verification and validation of the models has been carried out qualitatively using a dummy model and by looking at the increase of boundary layer thickness due to the rotation and comparing to matched cases found in literature.

1.9.2 Boundary Conditions

The CAD models have been imported into the CFD solver and the following boundary conditions have been assigned to the various faces:

- *Air Volume*: Freestream Inlet/Outlet
- *Helicopter Body Surfaces*: were subdivided in boundary walls for the following sections:
    - *Fuselage*
    - *Pods*
    - *Horizontal Tailplane*
    - *Vertical Fin*
- *Engine Inlet*: Mass Flow Outlet
- *Engine Outlet*: Mass Flow Inlet
- *Main Gear Box Inlet*: Mass Flow Outlet (only for CS27)
- *Main Gear Box Outlet*: Mass Flow Inlet (only for CS27)

- *Main Rotor Disc*: Actuator Disc
- *Main Rotor Mast*: <Not present>
- *Tail Rotor*: Actuator Disc
- *Tail Rotor Mast*: <Not present>

The settings related to the various boundary conditions have been determined during the CFD model validation phase, where several simulations have been performed and compared to the data provided by the CS29 reference helicopter TC HOLDER. The validated boundary condition types and settings are assumed to be suitable as well for the CS27.

1.9.3 Mesh Type

Mesh refinement volumes have been added all around the helicopter body to highlight aerodynamic effects in areas of interest:

- In the fuselage wake area
- Upstream of the horizonal and vertical tail plane
- Around the main rotor disc
- In the region affected by the hoist wake
- Around the HEFS pods
- At the engine inlet and outlet
- At the main gear box inlets and outlets (CS27)

Wall surfaces of the Helicopter body have been provided with boundary prism layers so that the wall $y^+ < 1$ everywhere on the helicopter surfaces. The helicopter is usually subjected to a turbulent airflow with a Reynolds Number $Re > 10'000'000$. We therefore expect the development of a turbulent boundary layer which requires a very thin -in the order of decimals of millimeter- prism layer thickness on the cell near the wall. No wall functions are used at the walls as the y+ is sufficiently small.

1.9.4 Physical Model

The CFD simulation is based on a RANS steady-state solver for incompressible, isothermal, turbulent flow called SimpleFOAM. This solver is widely used in external subsonic aerodynamic simulations and has been proved to be a robust algorithm in various aerospace applications. We must clarify two aspects:

- The local Mach number at the blade tip is not resolved as we are not interested in capturing the aerodynamic behavior of the rotor blades.
- The hot gas that exits the engine exhaust pipe is modelled as a simple mass flow without elevated temperatures. This approximation is suitable for simulations where the gas expansion is not primarily used to generate aerodynamic forces, which is the case for turboshaft engines used on helicopters.

The K-ω SST (Shear Stress Transport) turbulence model has been used. This turbulence model has been shown to be capable of capturing recirculation areas and flow detachment on bluff bodies to some extent. It should be noted that two equation turbulence models such as the K-ω SST typically underestimate the recirculation areas slightly and flow detachment on bluff bodies is not always correctly modelled. However, the K-ω SST (Shear Stress Transport) model is one of the two equation turbulence models which performs better compared to the others. The next level of physically correct turbulence modelling after the two equation K-ω SST model is Detached Eddy Simulation (DES), which is however computationally very demanding, and thus not compatible with the resources available in the current study.

The virtual time step of the simulation was set so that the $Courant\ Number < 0.5$ everywhere in the simulation domain. Sufficient convergence of the numerical equations for engineering purposes have been judged based on the convergence history of integrated coefficients such as mass flow rates, forces and pressures. In cases where fluctuations of the integrated coefficients around a horizontal average were observed which were most likely related to the unsteady nature of the real flow, sufficient convergence of the numerical equations for engineering purposes were determined.

1.9.5 Data Extraction

A data analysis framework between Python, Linux and the postprocessing tool ParaView has been established and used both for the CS29 and CS27 analyses. Data was automatically extracted from the simulations and routines have been used to analyse the data and provide the information needed.

1.10 Main Assumptions and Simplifications

Depending on complexity imposed on the numerical model (CFD), simplifications and assumptions have been applied to the framework. Two high level choices are important to note, applicable both to the CS29 and the

CS27 analysis:

- A detailed analysis is performed for the aerodynamic implications mentioned in section 1.1. By applying a delta analysis, major concerns can be flagged by looking at quantified deltas.
- A high-level analysis is performed of the aerodynamic effects mentioned in section 1.2. By applying a delta analysis based on qualitative results, concerns can be flagged.

1.10.1 Helicopter as a rigid body without landing gear

For the scope of this analysis the helicopter has been considered an infinitely rigid body and no aeroelastic effects have been considered. As agreed with EASA, the CFD framework used for the aerodynamic analysis of the CS29 did not include the Hoist nor the Landing gear. Drag contributions induced by the landing gear have been separately taken into account in the post-analysis after the CFD simulations. The CFD framework used for the aerodynamic analysis of the CS27 includes the skid.

1.10.2 Modelling of the engine and main gear box

For the scope of this analysis, the engine is not modelled into detail, but the effect of the in- and outflow is taken into account. As such, the engine is only modelled by giving a uniform mass flow out of the aerodynamic domain at the engine inlet, and a uniform mass flow into the domain at the engine outlet. The air mass flow through the main gear box inlets and outlets of the CS27 reference helicopter is modelled as well. All mass flows depend on the flight condition which is modelled and estimated by using typical engine characteristics.

1.10.3 Modelling of the main- and tail rotor

The MR and TR control chain and control positions have not been considered for the scope of this study. While flying, the helicopter must be in equilibrium conditions and the MR and TR should generate defined forces and moments around the HC principal inertia system, irrespective of the control chain which generate those forces.

It is also realistic to consider that the presence of the HEFS will not induce substantial changes to the main rotor behaviour at any speed in the flight envelope analysed:

- *No flapping motion induced in the MR blades*: As the pod is very close to the MR blades root, no dynamic stall is expected to be induced at the blade tip, neither any torsional forces or flapping propagation along the blades.
- *No change in the resonating frequencies at the main rotor mast*: The HEFS pod will experience a 4/rev vibration frequency (4-bladed rotor), so no change in the excitation spectrum is expected.

The study aims at capturing the delta of performance of the helicopter with HEFS with respect to the baseline helicopter. Since the rotor is not expected to change its macroscopic aerodynamic behaviour, the rotor parameters have been kept fixed for the scope of the analysis. It is assumed for the CS27 reference helicopter, that the tail rotor is not active when flying at the simulated speeds of 80, 110 and 140 kts. Hence, the actuation disk for the tail rotor of the CS27 reference helicopter is not active in the CFD simulations performed. This assumption is based on the fact that the CS27 reference helicopter has a fenestron ('fan-in-fin') with a significant rudder placed on the shroud. In forward flight, the effectiveness of the fenestron decreases a lot, where the rudder takes over to counter the torque induced by the main rotor and relieve the fenestron. In forward flight, the power consumed by the fenestron can be assumed to be close to zero (Huot, 2013).

1.10.4 Handling Quality Assessment

It is assumed that when the presence of the HEFS doesn't cause the helicopter flying characteristics to be outside of the limits defined in section 1.6, the handling qualities are sufficiently similar as the handling qualities of the baseline helicopter. It is assumed that within these limits the autopilot compensates for the changes, without recertification (autopilot) or significant training (type rating). For the CS27 reference helicopter, the same directive is used, which is expected to be a conservative approach (stability margins for the CS27 are expected to be more flexible compared to the CS29).

Important to note is that for the assessment of the handling quality:

- In post-processing of the CFD data, a semi-articulated rotor is assumed both for the CS29 and CS27 reference helicopter. This assumption influences the static margins of the helicopter estimated using equations from literature.
- No evolution of the Main Rotor dynamic model, hence the oscillations captured in the following analysis only describe the proper oscillations of the fuselage. The simplification of this assumption is sufficient for our purposes since the rotor starts reacting with some time delay and for small attitude variations at the beginning of the oscillation it can be considered static.

2. Validation of CFD Model

The validation of the CFD framework has been performed by comparing simulation results with data provided by the reference helicopter TC HOLDER and open source data. The validation was performed using the CS29 reference helicopter, since for this most validation data was available.

2.1 Available Validation Data provided by TC HOLDER

2.1.1 Quantitative data CS29

The quantitative data referred to the CS29 reference helicopter flying in medium take-off-weight (5900 kg) and mid-CG longitudinal configuration. The data applied to SSL at ISA atmospheric conditions. The plot in Figure 9 shows the interpolated drag data and furthermore for each calibrated airspeed, the following quantitative data was available for the project.

- MR Torque
- MR Thrust
- Alpha Tip Path Plane (with respect to fuselage z direction, positive is disk pointing forward)
- Fuselage Pitch
- Fuselage Roll
- Helicopter Body Drag (*including Fuselage, Horizontal Stabilizer and Vertical Fin)

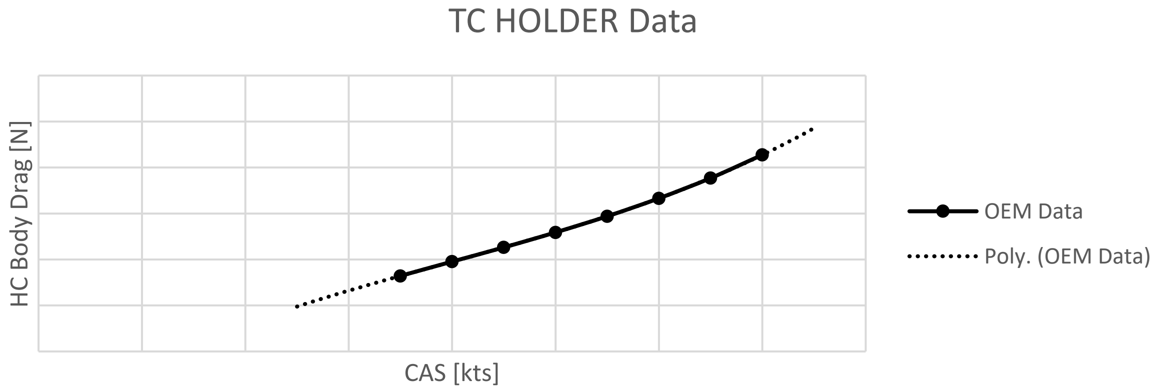

Figure 9 Drag data provided by TC HOLDER and interpolated with Polynomial spline

2.1.2 Qualitative data CS29

The qualitative data provided by the TC HOLDER included images extracted from a CFD solver presenting:

- the distribution of pressure coefficient over the helicopter fuselage
- the distribution of pressure coefficient projected onto a symmetry plane

2.1.3 Quantitative data CS27

An approximation of the RPM of the CS27 reference helicopter has been made based on data related to the CS29. By keeping a consistent blade tip speed to the CS29 reference helicopter, it has been possible to estimate the rotational speed of the CS27 reference helicopter Main Rotor. The attitude (pitch and roll angle) has been estimated using flight mechanics equilibrium conditions and approximating the fuselage down lift.

The CS27 reference helicopter TC HOLDER provided information about the CG location and provided the power curve shown in Figure 10.

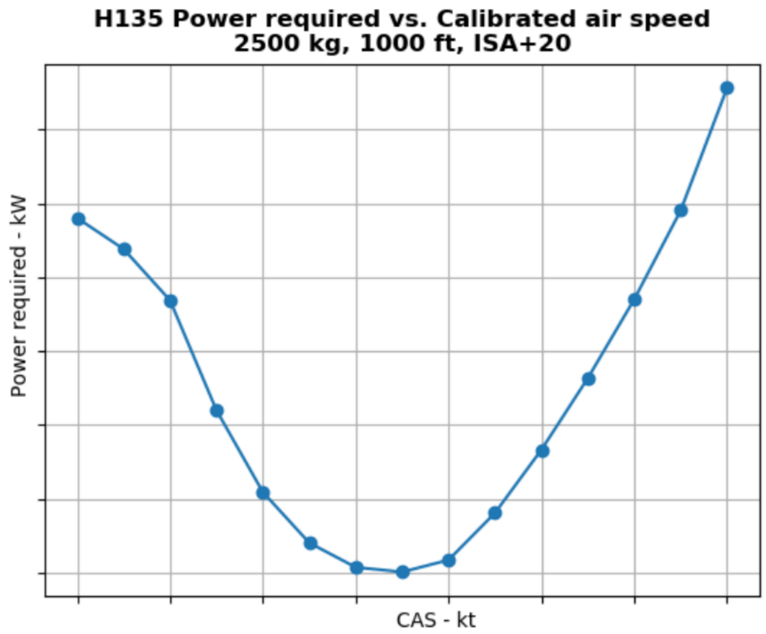

Figure 10 CS27 reference helicopter power curve provided by TC HOLDER

2.2 CFD Validation Strategy and Results

2.2.1 Validation Strategy

The validation of the CFD model has been based on three strategies:

- *Qualitative matching of aerodynamic data*: The CP distribution both in the symmetry plane and on the helicopter's surface must be similar to the one provided by the TC HOLDER. Differences in CAD models must be considered, however the pressure distribution on key areas must show similar trends.
- *Quantitative drag approximation*: The value of the drag obtained in the CFD model must match the drag value provided by the TC HOLDER. The study must identify the importance of specific simulation settings and fine tune those till matching the reference data as much as possible.
- *Expert interpretation of physical quantities*: The airflow simulated must show realistic absolute values, especially in the boundary layers which are generated at the walls.

2.2.2 Mesh and Numerical Model

The meshing software used was CfMesh, the software comprises automatic meshing workflows and the implemented methodology can generate very large and complex unstructured volume meshes built according to the so called inside-out process. Prism layers are extruded from the surfaces and cells are removed or reshaped as the layer grows. The mesher requires a high quality input model and cannot mesh sharp edges and cavities. For this reason, every edge in the model has been filleted according to the local mesh size. Refinement regions have been defined around the helicopter and on the helicopter wake. The boundary layer has been set to guarantee a y+ < 1 in all the regions where Re < 500'000. The surface mesh size has been imposed by the size of details to be kept in the simulation. The total number of cells has resulted in approximately 15M cells.

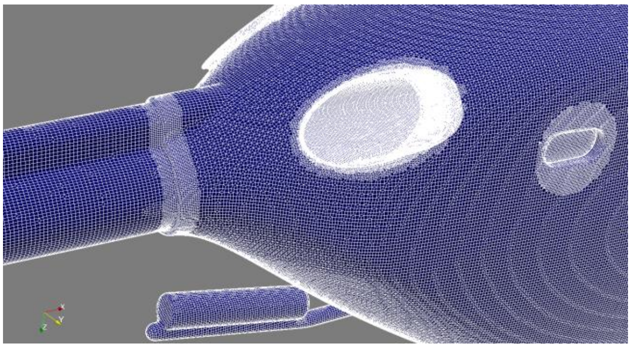

Figure 11 Surface mesh refinement

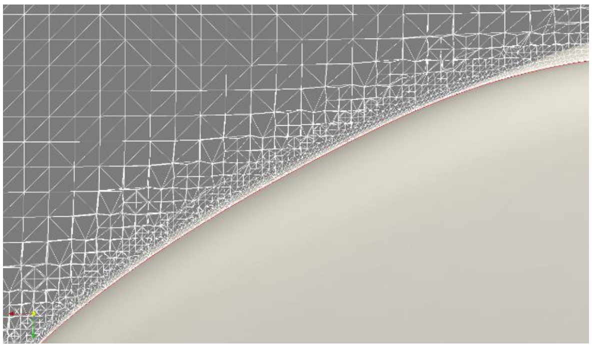

Figure 12 Boundary layer prism mesh transition

The settings used in OpenFOAM are summarized in Table 3.

Setting	Selected
Simulation type	RANS – Simple Algorithm
Turbulence model	K-Omega SST

Table 3 CFD numerical model

2.2.3 Selection of Physical parameters

Turbulence is mainly governed by two parameters: k and ω. The final selection of the right parameters to be used in the boundary conditions and initial conditions has followed an iterative approach, based on the evaluation of the sensitivity of the single parameters and the application of a scaling factor to the calculated values of both k and ω in order to match the drag of the helicopter as provided by the TC HOLDER. It can be seen from Figure 13 how the choice of a scaling factor of ω is the parameter with most influence on the results. The use of different discretization schemes like *Upwind* and *Linear-Upwind* and the choice of y+ < 1 or y+ < 2 do not significantly influence the drag of the helicopter. For k at the walls a value near 0 (i.e. 1e-12) was used, as the turbulent kinetic energy near the walls is (almost) zero. An upwind discretization scheme is selected.

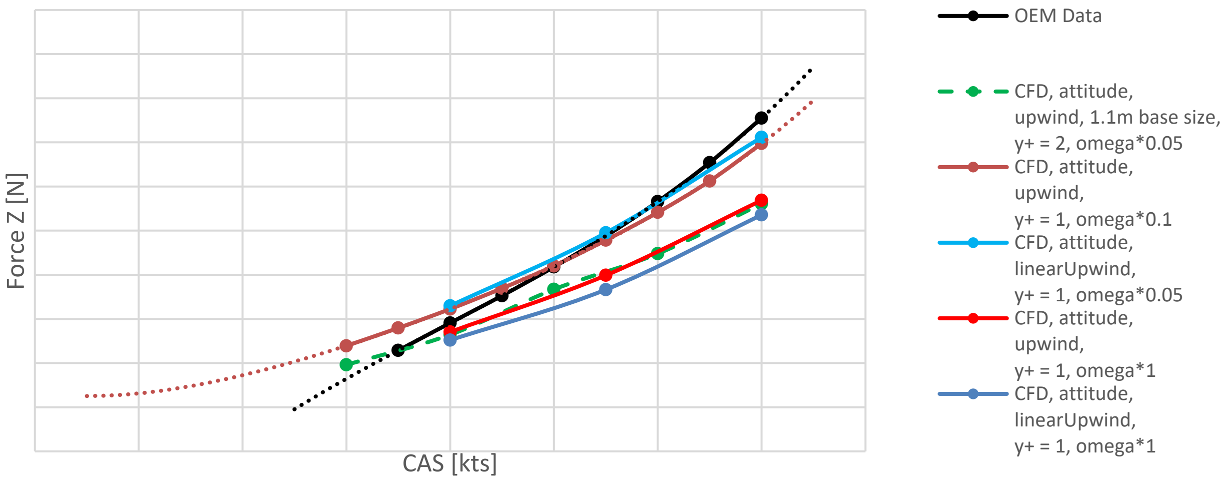

Figure 13 Reference drag compared to the drag according to different turbulence parameter values

The images below show a pressure distribution around the CS29 reference helicopter that practically match the data provided by the TC HOLDER. Similarities are present along the fuselage and on the frontal fuselage and frontal cowling areas. Differences can be identified on the engine inlet as the CAD model used has a more accurate engine inlet geometry.

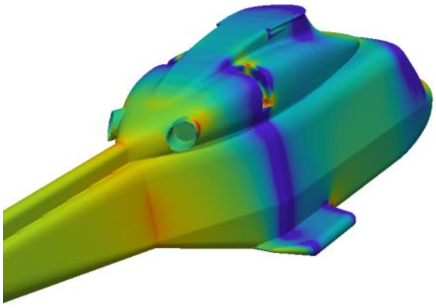

*Figure **14** OpenFOAM CS29 Reference Helicopter airflow static pressure*

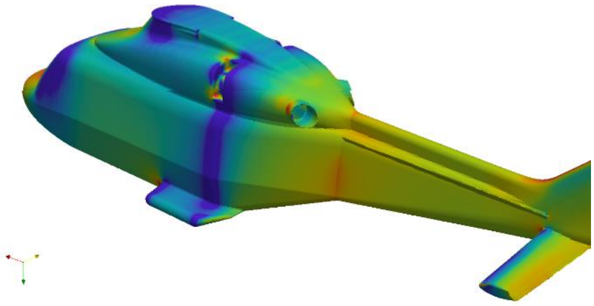

*Figure **15** OpenFOAM CS29 Reference Helicopter airflow static pressure*

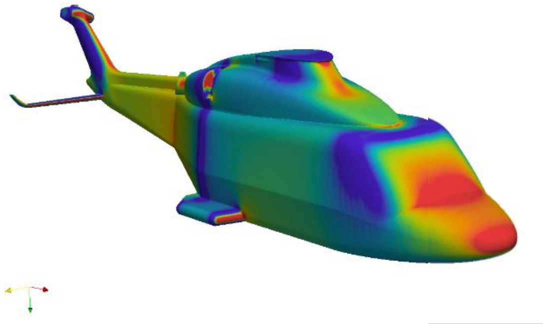

*Figure **16** OpenFOAM CS29 Reference Helicopter airflow static pressure*

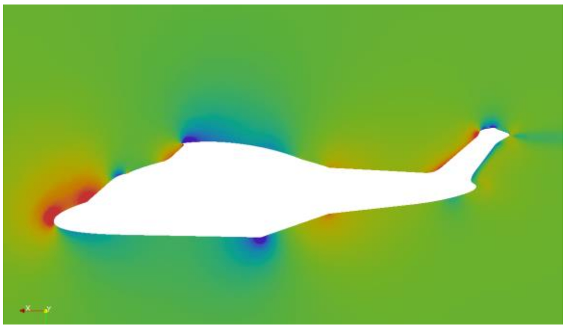

*Figure **17** OpenFOAM CS29 Reference Helicopter airflow static pressure*

The boundary layer can be easily displayed by plotting the turbulent viscosity ν_t (nu_t). The boundary layer appears as a red region in the image below all around the helicopter fuselage.

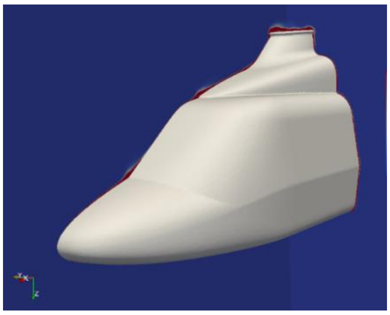

*Figure **18** OpenFOAM Projection of $\boldsymbol{\nu_t}$ on cross sections*

The wake propagation behind the tail is displayed below and resembles a realistic wake dissipation.

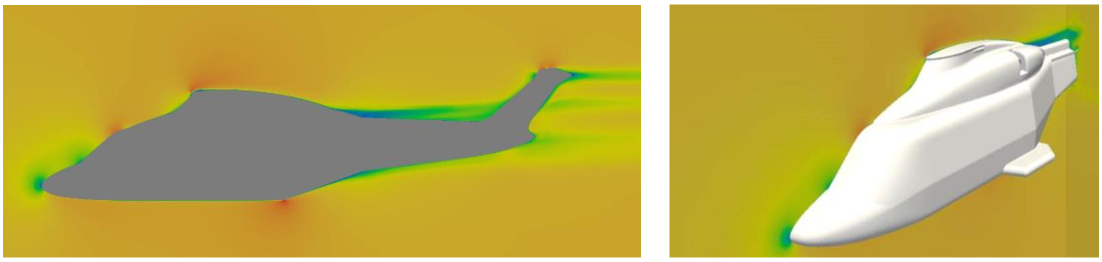

*Figure **19** OpenFOAM Velocity field in cross section*

2.2.4 Physical Quantities Check

Accuracy of the results are dependent on a correct characterization of the boundary layer and its flow physical quantities. The check involved the analysis of k and ω. The profile of k at wall matches literature data showing a pronounced peak of turbulent kinetic energy and it is well discretized in more than 8 discretization points.

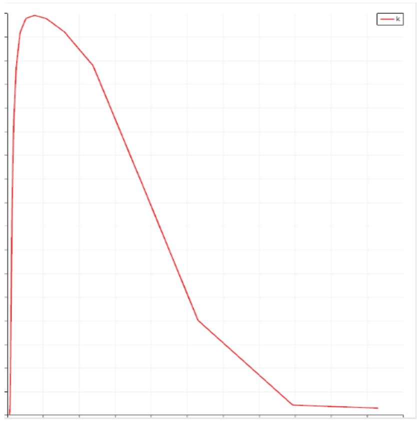

Figure 20 Extracted $\boldsymbol{k}$ profile at boundaries

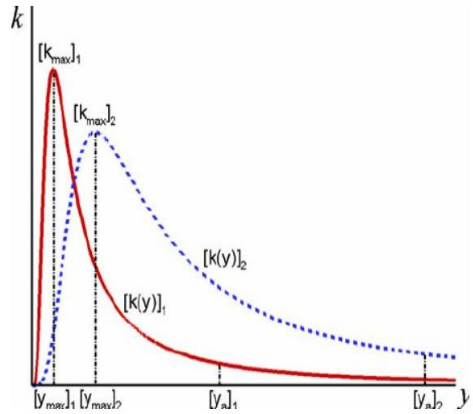

Figure 21 $\boldsymbol{k}$ profile according to experimental data from literature (Shur, Spalart, Strelets, & Travin, 2011)

The profile of omega approaches infinity as it gets closer to the wall. Given the limits of the numerical approaches, the value of omega reaches the order of 10^6.

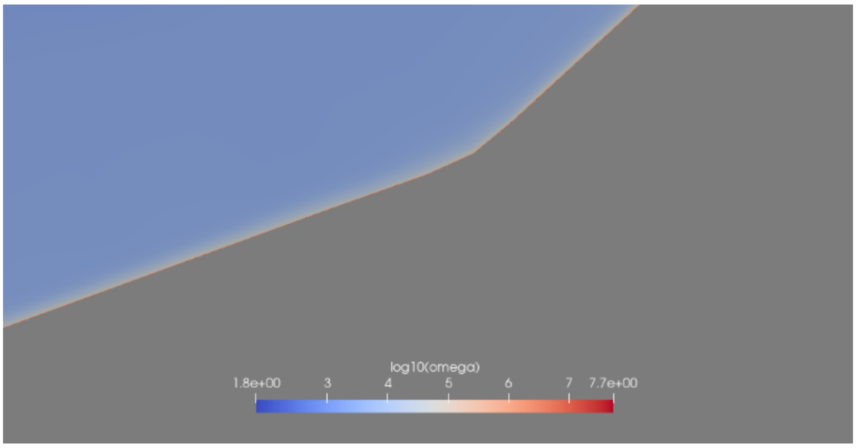

Figure 22 $\boldsymbol{\omega}$ approaches infinity as it gets closer to the wall

2.2.5 Quantitative Results CS29

Following the selection of parameters, the associated estimated drag is represented by the curve in Figure 23. The speeds of interest range from 70kts ($V_{climbout}$-10kts) to 140kts CAS (1.1 V_H). The maximum deviation of results is +25% in low speeds and -10% in high speeds. Drag versus speed is expected to follow a quadratic trend as the drag is proportional to V^2 and for these reasons, the differences between the 'TC HOLDER data' curve and the curve as obtained from the CFD model have been accepted and the model has been considered validated at a sufficient level for the scope of the study.

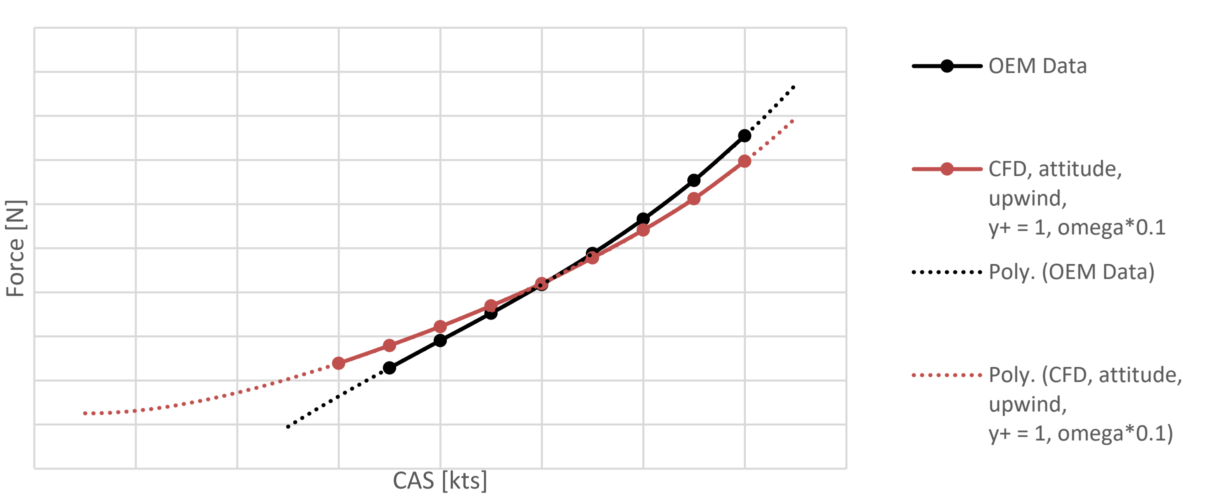

*Figure **23** Reference drag compared to the drag according to selected turbulence model*

3. Qualitative Aerodynamic Assessment and Pod Design

3.1 CS29 Reference Helicopter

The installation of the HEFS pods must not affect the normal safe operations of the CS29 reference helicopter. In particular, no unacceptable interference must arise between the HEFS pods and the various helicopter systems (such as engine components, rotor components, hydraulic system and autopilot and general electronic systems). Helicopters designed under CS29 certification standards are designed to operate in IFR navigation. Helicopters of this category are typically equipped with two identical engines and an Autopilot-SAS system for the offshore fleet. The design of the HEFS pods must consider the continuous correct functioning of these systems.

3.1.1 Geometric Constraints

The component should be designed in such a way that all the following requirements are met:

- The rotor does not touch the HEFS pods when blades at lowest flap in normal operative conditions
- The pod does not cover any existing critical sensors and components in the cowling area
- The pod does not have unacceptable interference with the engine inlet and various anti sand or anti-icing systems
- The pod does not cover any NACA inlets present on the cowling
- The pod covers the HEFS cylinder with sufficient geometrical margins to account for manufacturing tolerances
- The location of the HEFS cylinder is constrained by satisfying the requested buoyancy
- The location of the pod does not interfere unacceptably with normal helicopter maintenance.

3.1.2 CS29 Reference Helicopter Frontal Area

The frontal Area of the pods should be maintained as small as possible to reduce the drag coming from the helicopter body.

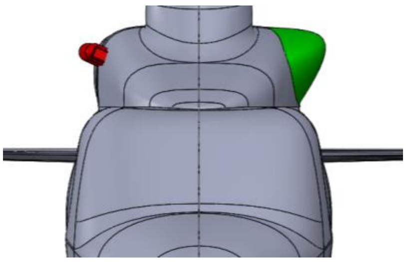

Figure 24 CS29 reference helicopter frontal area: with HEFS (Left) and with HEFS pod (Right)

The frontal area of the baseline helicopter without a hoist is $5.93m^2$. The introduction of pods on both sides of the helicopter increased the frontal area to $6.16m^2$, an increase of $+3.8\%$. In a first approximation one can assume that the drag of the helicopter body is in fact linearly dependent to the frontal area according to:

$$D_{fuselage+tail} \cong \frac{1}{2}\,\rho\,V^2\,C_{D0}\,S$$

This contribution includes the Form Drag and the Skin Friction Drag. We therefore expect an increase in the Helicopter Body Drag of an overall $+3.8\%$. We must also consider that the Helicopter body Drag usually contributes about 60% to the overall helicopter Drag, assuming a clean fuselage (no hoist, no landing gear). This is also confirmed by data provided by the TC HOLDER for medium take-off-weight (5900 kg).

This means that $+3.8\%$ is only accountable for a fraction of the overall drag. Table 4 provides an estimation of the overall Drag Increase due to the pods at the various CAS in forward flight.

TAS [kts]	Overall Drag Incr.
60	**+1.56%**
70	**+1.93%**
80	**+2.08%**
90	**+2.16%**
100	**+2.21%**
110	**+2.25%**
120	**+2.28%**
130	**+2.32%**
140	**+2.36%**

Table 4 Preliminary estimation Drag Increase due to pods in Forward Flight

Future phases of the study include also an estimation of the increase of operative costs as a consequence of the drag increase, which will be strictly related to the mission profile chosen.

For the data in the table above, the forward Thrust was used which has been obtained by the data provided by the helicopter TC HOLDER. The data included the MR thrust and the forward inclination of the main rotor, identified through the parameter α_{MR}, counted positive for forward inclination of the rotor TPP. The formula used to determine the forward thrust is:

$$T_{MR\,|\,fwd} = T_{MR}\ \sin(\alpha_{MR}) \tag{12.1}$$

Following the same principle, it is possible to estimate the ROC penalties. In the example below , the change in Rate Of Climb has been evaluated for the aircraft flight in forward flight, altitude SSL, mass 6400kg (taken as max take-off weight), extracted landing gears, no Hoist and with both engine working at MCP. Numbers must be confirmed by CFD simulations and by TC HOLDER but the table already provides insights of the effect of the ROC achievable in the case of the helicopter with HEFS in comparison to a baseline Helicopter.

TAS [kts]	ROC baseline HC [ft/min]	ROC HC+HEFS [ft/min]	ROC Decrement [%]
60	2187.325	2185.967	**-0.06%**
70	2245.785	2242.832	**-0.13%**
80	2182.97	2177.965	**-0.23%**
90	2057.394	2049.94	**-0.36%**
100	1934.371	1923.953	**-0.54%**
110	1685.033	1671.039	**-0.83%**
120	1325.206	1306.874	**-1.38%**
130	873.5192	849.9032	**-2.70%**
140	282.4836	252.4149	**-10.64%**

*Table **5** Rate of Climb Impact Estimation*

3.1.3 CS29 Reference Helicopter Vertical Area

The Vertical Area of the Pod should be evaluated in a direction perpendicular to the main rotor TPP when the helicopter is hovering Out of Ground Effect (HOGE).

Also in this case, the overall increase of area should be kept as small as possible, and the HEFS pods be positioned in the vicinity of the Main Rotor mast, where the rotor inflow is at the minimum. As it is possible to see from Figure 25, the increase in vertical area is almost null and therefore we do not expect a significant increase in vertical Down-Lift In HOGE. Following the same principle, we do not expect any degradation in maximum achievable vertical ROC.

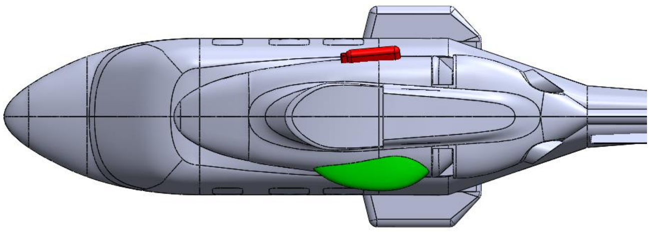

Figure 25 Top View: Helicopter CS29 with HEFS (above) and Helicopter with HEFS pod (Below)

3.1.4 Longitudinal Stability

The reference helicopter operates SAR missions where it is required to keep a Position Hold HOGE. The hoist operator must direct the cable anchor at the desired location while the Autopilot System provides high stability and controllability to the helicopter. SAR autopilot modes are usually very sensitive to constant disturbances of steady entity and the actuators in the control chain are operating at their maximum controlling power.

The introduction of the HEFS pods must not introduce forces in longitudinal direction parallel to the ground and no moments around the body y axis. The shape of the pods should be designed in such a way that no forces and moments are generated in the longitudinal vertical plane.

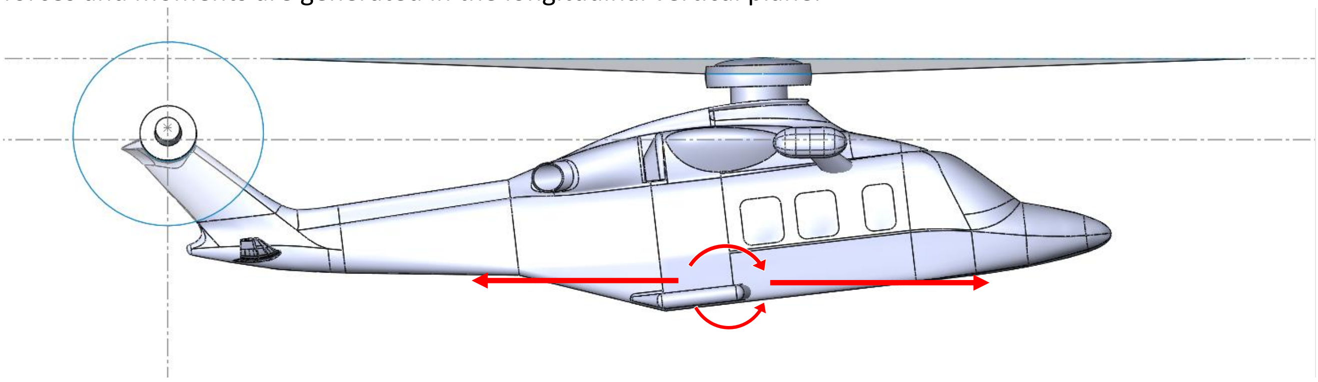

Figure 26 Schematics of the forces and moments that should be avoided in longitudinal direction

One of the possible solutions to not create forces and moments is to design symmetric pods, with the symmetry plane oriented perpendicular to the TPP. The helicopter manufacturer provided the information of the Helicopter Pitch at various CAS and in HOGE. In HOGE the helicopter fuselage presents a nose up attitude that has been taken into account during the design the pods. The Main Rotor, on the other hand, remains horizontal to the ground in HOGE.

As it is possible to see from Figure 27, the pod is oriented parallel to main rotor TPP, the same orientation of the hoist main body.

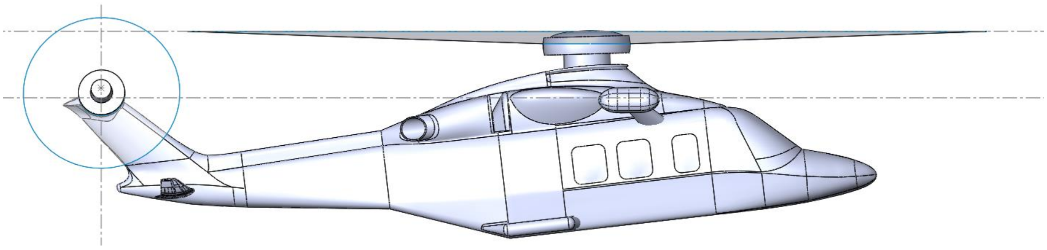

Figure 27 Rotor TPP, Hoist hull and HEFS pod parallel to local horizontal plane

The adoption of a symmetric pod configuration, both on the left and the right side of the fuselage, should ensure that no forces are created in the lateral direction.

3.1.5 Vortex Shedding and Engine Inlet Disturbances

The constrained spaces in which the pod must be placed could potentially induce separation of the flow in the trailing part of the pod. The shedding of vortices originating from the recirculation area might create vibration to the fuselage side. Taking into account the design rules defined in the paragraphs above, the pods must be designed as streamlined as possible, offering a good slope for pressure recovery both in the vertical direction (useful during Hover conditions) and in horizontal direction (for level horizontal flight conditions) to avoid extreme vortex shedding. For this helicopter, the position of the engine inlet might represent a constraint for the design of the pods. The blunt body hull placed in front of the engine inlet might introduce turbulence at the engine inlet vane. For this reason, the pod shape shall be streamlined as much as possible and shall not induce flow separation at the engine inlet vane.

3.1.6 Comparison to Similar Certified Modifications

In order to create some perspective on the aerodynamic impact of the installation of the pods, for comparison some examples are given below of existing intrusive installations on the fuselage of CS29 certified helicopters:

- Hoist
- Bubble windows
- Ice detector
- Cable cutter
- Searchlight
- Imaging system

The hoist installation is most comparable to the HEFS pods because of the similar location of installation on the fuselage (upper cowling). When comparing the installation of the HEFS pods to the - already certified - installation of a hoist it can be expected that the aerodynamic impact of the HEFS pods on CS29 certified helicopters will be less intrusive compared to that of the hoist. This can be related to the fact that the HEFS pod design will be symmetrical and will for most helicopter types result in a smaller increase in frontal area compared to the hoist installation.

3.1.7 Preliminary Conclusion CS29

Based on the qualitative design review, the aerodynamic impact is not expected to induce significant aerodynamic penalties:

- In the range of 50-60knots: increase of helicopter body drag in forward flight of +1.5% and decrease of ROC almost non-existent. The helicopter usually crosses this speed over the runway and the data demonstrates that no impact on the take-off phase is present.

- In the range of 70-90knots: increase of helicopter body drag in forward flight of +2.3% and decrease of ROC almost non-existent. The helicopter can reach the expected ROC and to accomplish any realistic mission profile, even in OEI.

It has been possible to define a geometry for the pods that reduces flow separation and has a relatively benign frontal and vertical area impact. The same geometry design can be used to create HEFS pods for any other aircraft, while the same aerodynamic considerations apply to helicopters of both CS27 and CS29 certification types. The HEFS pods symmetric design is not expected to produce static instability effects on the lateral direction or in yaw motion. Moreover, by designing pods which have a symmetry plane perpendicular to the MR TPP in hover, we also expect no changes to the longitudinal stability and cyclic trim in HOGE. In forward flight, the small increase in frontal area will induce an increase of drag as shown in Table 4, which translates to an increase in fuel costs. The location of the HEFS pods close to the MR mast, will not induce significant dynamic effect on the MR blades and it is not expected to reduce the performance of the MR disc. Also, the location of the HEFS pods in the vicinity of the helicopter CG, will not induce aerodynamic moments that can significantly modify the helicopter static and dynamic stability. The CFD simulations will be used to generate data to further validate this assumption. Finally, when comparing the installation of the HEFS pods to similar – already certified – installations such as a hoist, the impact of the HEFS pods is expected to be smaller, based on the symmetrical design and a comparable or smaller increase in frontal area.

3.2 CS27 Reference Helicopter

The installation of the HEFS pods must not affect the normal safe operations of the CS27 reference helicopter (Airbus EC135). No unacceptable interference must arise between the HEFS pods and the helicopter systems such as the engine components, rotor components and, if available, the autopilot. Helicopters designed under CS27 certification standards are not necessarily designed to operate under the IFR, which means that some CS27 type helicopters only fly under VFR. In addition to this, there is not always a Stability Augmentation System (SAS) or Automatic Flight Control System on board. Helicopters in this category are typically equipped with two identical engines for the offshore fleet. For the qualitative analysis presented in this section, a preliminary design of the HEFS pod has been defined, making sure the pod complies with geometrical constraints while at the same time it has an aerodynamic design.

3.2.1 Geometric Constraints

The aerodynamic pod covering the HEFS component should be designed in such a way that all the following requirements are met:

- The rotor does not touch the HEFS pods when blades at lowest flap in normal operative conditions
- The pod does not cover any existing critical sensors and components in the cowling area
- The pod does not have unacceptable effect on the engine inlet airflow and various anti sand or anti-icing systems
- The pod does not cover any inlets or vents present on the cowling
- The pod covers the HEFS cylinder with sufficient geometrical margins to account for manufacturing tolerances
- The location of the HEFS cylinder is constrained by satisfying the requested buoyancy requirements

- The location of the pod does not interfere unacceptably with normal helicopter maintenance.

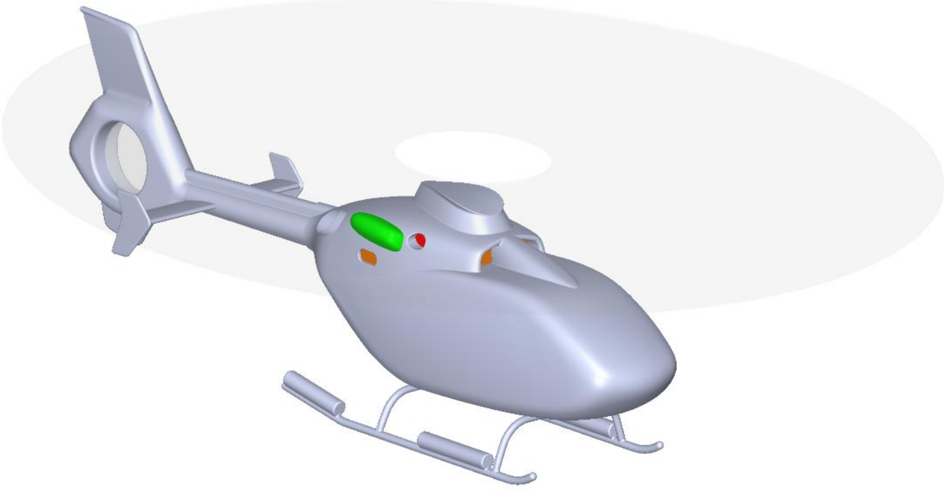

Figure 28 CS27 including preliminary pod design in green

As can be seen from Figure 29, the design freedom of the pod shape is very limited for the CS27 reference helicopter due to the geometric constraints. The space between the air vents coloured in orange (air inlets) and red (air outlets) is limited, causing the pod (presented in green) to be a blunt shape rather than aerodynamic, covering the uninflated HEFS system with small margins.

3.2.2 CS27 Reference Helicopter Frontal Area

The frontal Area of the pods should be maintained as small as possible to minimise the extra drag adding to the existing the helicopter body drag. The frontal area, excluding the skids, of the baseline reference helicopter without a hoist is $3.3m^2$. The introduction of pods on both sides of the helicopter increases the frontal area to

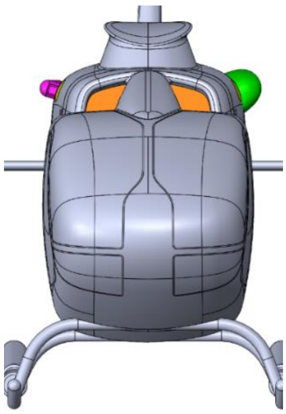

$3.38m^2$, an increase of $+2.5\%$.

In a first approximation one can assume that the drag of the helicopter body is in fact linearly dependent to the frontal area according to:

$$D_{fuselage+tail} \cong \frac{1}{2}\,\rho\,V^2\,C_{D0}\,S$$

Figure 29 CS27 reference helicopter frontal area: with HEFS (Left) and with HEFS pod (Right)

This contribution includes the body Form Drag and the Skin Friction Drag. We therefore expect an increase in the Helicopter Body Drag, excluding the effect of the skids, of $+2.5\%$. We must consider that the Helicopter Body Drag is only a part of the overall helicopter drag, where a few other terms also contribute. This means that the drag increase of the overall helicopter drag caused by the pods, will be smaller than 2.5% since the additional contributions of the Main Rotor and Tail Rotor drag, the skids and the hoist will be added.

3.2.3 CS27 Reference Helicopter Vertical Area

The Vertical Area of the Pod should be evaluated in a direction perpendicular to the main rotor TPP when the helicopter is hovering Out of Ground Effect (HOGE).

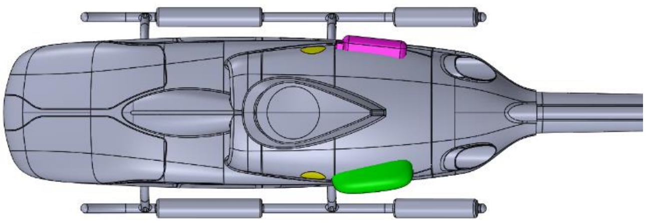

Figure 30 Top View: Helicopter CS27 with HEFS (above) and Helicopter with HEFS pod (below)

Also in this case, the overall increase of area should be kept as small as possible, and the HEFS pods be positioned in the vicinity of the Main Rotor mast, where the rotor inflow is at the minimum. As it is possible to see from Figure 31, the increase in vertical area is very small and therefore we do not expect a significant increase in vertical Down-Lift In HOGE. Following the same principle, we do expect a minimal degradation in maximum achievable vertical ROC.

3.2.4 Longitudinal Stability

The reference helicopter can operate SAR missions where it is required to keep a Position Hold in HOGE. The hoist operator must direct the cable anchor at the desired location while the Autopilot System provides high stability and controllability to the helicopter. SAR autopilot modes are usually very sensitive to constant disturbances of steady entity and the actuators in the control chain are operating at their maximum controlling power. The introduction of the HEFS pods must not introduce forces in longitudinal direction parallel to the ground and no moments around the body y axis. The shape of the pods should be designed in such a way that no forces and moments are generated in the longitudinal vertical plane, see Figure 31.

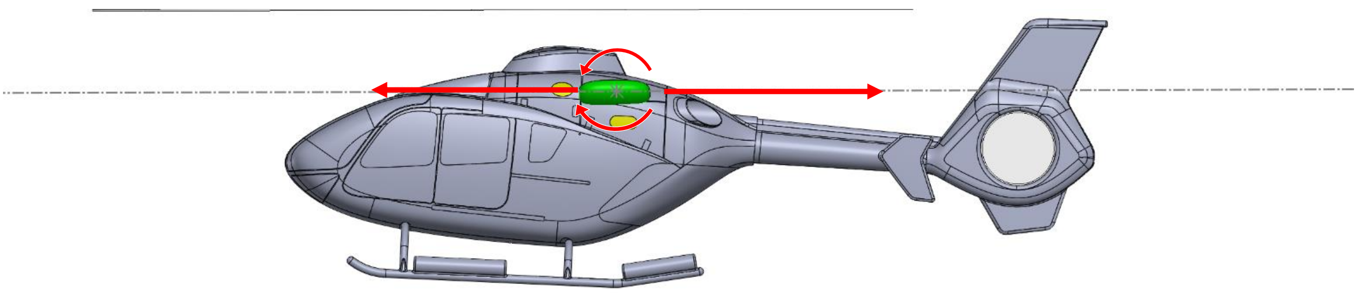

Figure 31 Schematics of the forces and moments that should be avoided in longitudinal direction

3.2.5 Vortex Shedding and Engine Inlet Disturbances

The constrained spaces in which the pod must be placed causes limitations to the freedom of pod design. The preliminary design of the pod for the CS27 reference helicopter, is more blunt rather than aerodynamic (such as the design for the CS29 reference helicopter). The blunt pod design might cause a limited pressure recovery both in the vertical direction and in the horizontal direction. This may potentially induce quite a large separation of the flow in the trailing part of the pod. The shedding of vortices originating from the recirculation area might create vibration to the fuselage. For this particular helicopter, the position of the engine inlet might represent a constraint for the design of the pods. The blunt body hull placed on top of the engine inlet might introduce turbulence at the engine inlet vane especially at low speeds. For this reason, the pod sizes should be kept as small as possible, to avoid induced flow separation at the engine inlet vane.

3.2.6 Comparison to Similar Certified Modifications

In order to create some perspective on the aerodynamic impact of the installation of the pods, for comparison some examples are given below of existing intrusive installations on CS27 certified helicopters:

- Hoist
- Ice detector
- Flotation devices on skids
- Cable cutter
- Searchlight
- Imaging system

The hoist installation is most comparable to the HEFS pods because of the similar location of installation on the fuselage (upper cowling). When comparing the installation of the HEFS pods to the - already certified - installation of a hoist it can be expected that the aerodynamic impact of the HEFS pods will be less intrusive compared to that of the hoist. This is because the HEFS pod design will be symmetrical and will for most helicopter types result in a similar or smaller increase in frontal area compared to the hoist installation.

3.2.7 Preliminary Conclusion CS27

Based on the qualitative design review, the aerodynamic impact may create some aerodynamic consequences, partly because of the limited design space imposed by the geometrical constraints. These limitations in design freedom of the pods cause the (preliminary) pod design for the CS27 to be a blunt shape rather than aerodynamic. Compared to the CS29 pod design, the pod for the CS27 may induce more flow separation and consequently vortex shedding. The increase in frontal area caused by the pods will cause an increase in helicopter body drag, excluding skids and rotors and hoist, of around 2.5%. Since the skids have a very large contribution to the overall drag and we must also consider the drag from the main rotor, the tail rotor and the hoist, the total increase of overall helicopter drag caused by the pods is approximated to be less than 1%. The HEFS pods symmetric design is not expected to produce static instability effects on the lateral direction or in yaw motion. Moreover, by designing pods which have a symmetry plane perpendicular to the MR TPP in hover, we also expect negligible changes to the longitudinal stability and cyclic trim in HOGE.

The location of the HEFS pods close to the MR mast, is not expected to induce significant dynamic effects on the MR blades and it is not expected to reduce the performance of the MR disc. Also, the location of the HEFS pods in the vicinity of the helicopter CG, will not induce aerodynamic moments that can significantly modify the helicopter static and dynamic stability. The CFD simulations will be used to generate data to further validate this assumption. Finally, when comparing the installation of the HEFS pods to similar – already certified – installations such as a hoist, the impact of the HEFS pods is expected to be smaller, based on the symmetrical design and a in comparison similar or smaller increase in frontal area.

4. Quantitative Aerodynamic Assessment CS29

4.1 Reference System

Figure 32 shows the sign convention and definition of the longitudinal cyclic input. The reference system used in the quantitative aerodyanamic assessment is presented in Figure 33.

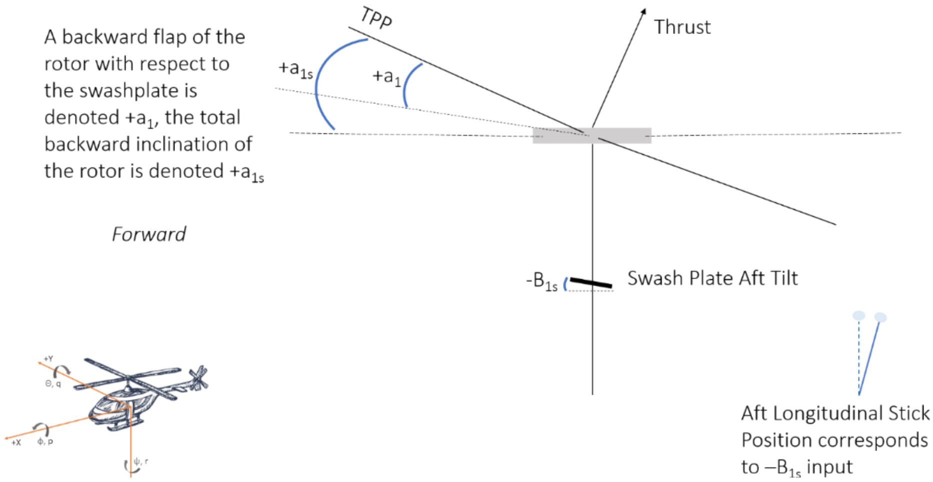

Figure 32 Definition and sign convention of longitudinal cyclic input B_{1s}

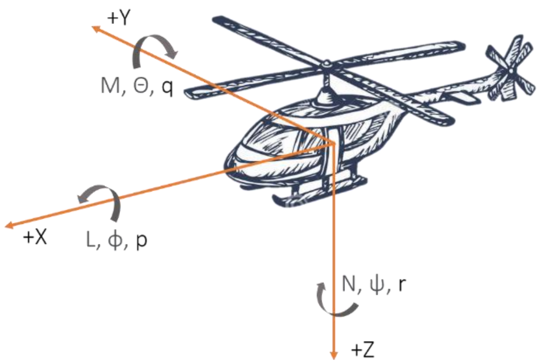

Figure 33 Helicopter Reference System

4.2 Wake and Vortex Shedding Analysis

4.2.1 Wake Cross-Sectional Area

A delta analysis (with and without the pod) has been conducted, inspecting the cross-sectional area of the wake behind the helicopter to see what effect the HEFS pods have on the wake propagation. For this, two flight speeds have been analysed, 110 kts and 60 kts. As the results from flight condition 2 are very similar to the results from flight condition 1, only the results from condition 1 are presented.

In **Error! Reference source not found.** and **Error! Reference source not found.**, cross-sectional planes are presented of the wake of the base model and the model including HEFS pods, visualizing the velocity in the x direction (longitudinal to the helicopter). Most of the disturbance seen in the wake is caused by the exhaust flow from the engine outlet. Slightly above and to the left of the right engine in **Error! Reference source not**

found. at the very start of the wake a larger disturbance is observed for the model including the HEFS pods. This larger disturbance is directly downstream of the pods and is most likely the wake of the pods. Propagating further into the wake, this extra disturbance due to the pods can still be observed in the upper part of the wake, however the disturbances caused by the exhaust flow from the engine dominate the wake. In conclusion, the HEFS pods cause some extra disturbance in the wake downstream of helicopter, causing the wake to be slightly more extended upwards.

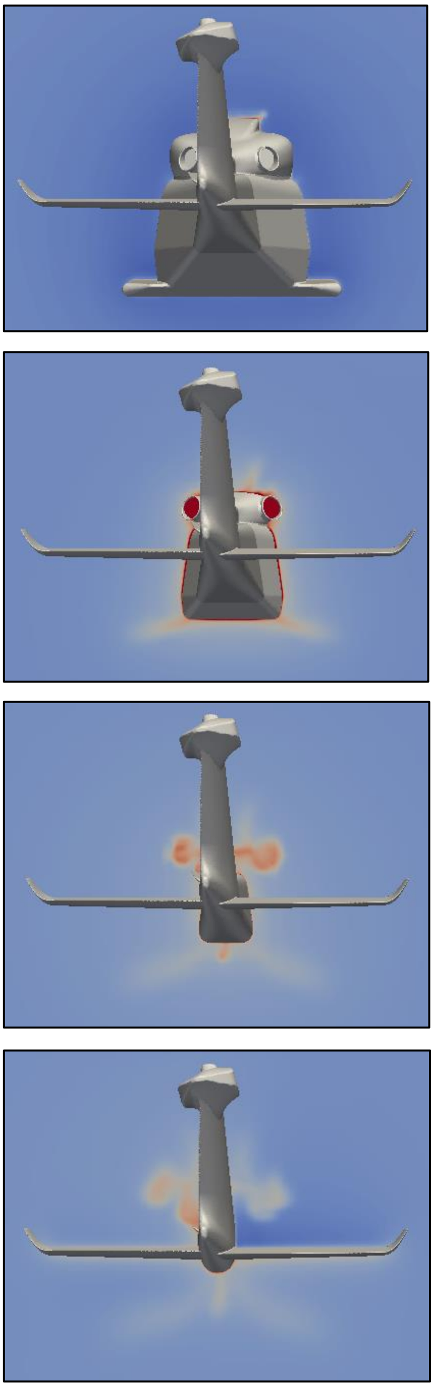

Figure 34 Wake propagation (U_x [m/s]) CS29 baseline reference helicopter at 110 kts

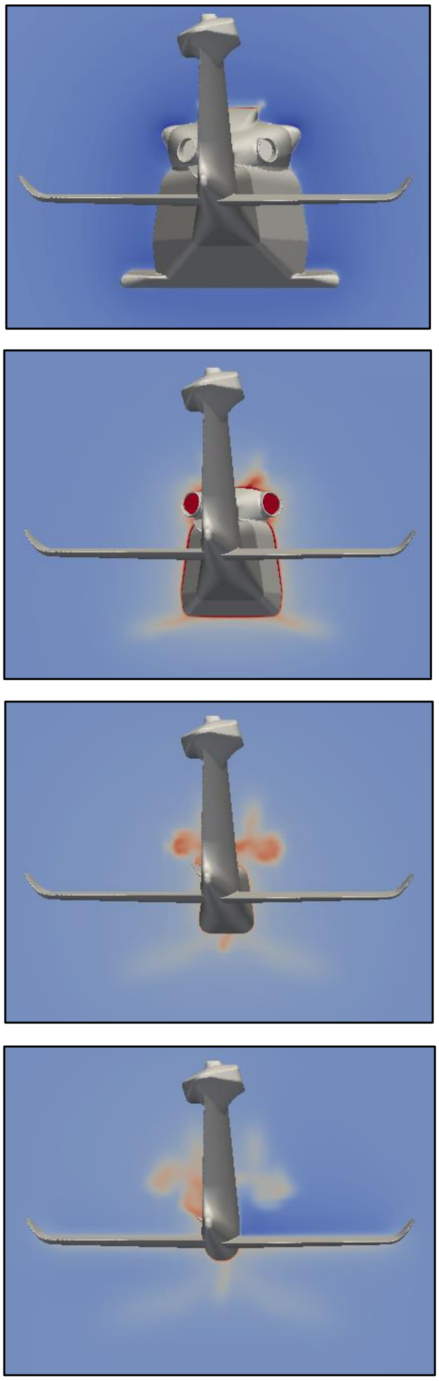

Figure 35 Wake propagation (U_x [m/s]) CS29 reference helicopter including pods at 110 kts

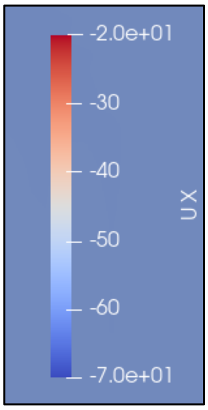

4.2.2 Vortex Shedding from Pod

An analysis has been conducted of the vortex shedding frequency of the HEFS pods, using the Strouhal relation. This analysis has been performed for two flight speeds, 110 kts and 20 kts. For the two conditions for which the shedding frequency of vortices has been analysed, the local Reynolds numbers at the HEFS pods are presented below.

$$Re_{110kts} = \frac{V\,L}{\nu} = \frac{56.59 \cdot 1.6}{1.5 \cdot 10^{-5}} = 6.04 \cdot 10^{6}$$

$$Re_{20kts} = \frac{V\,L}{\nu} = \frac{10.29 \cdot 1.6}{1.5 \cdot 10^{-5}} = 1.10 \cdot 10^{6}$$

The following Strouhal numbers apply to the different flight conditions:

$$St_{110kts} \approx 0.25$$
$$St_{20kts} \approx 0.24$$

The relation for the Strouhal number can then be used to approximate the shedding frequency of vortices from the pods. Here, D is the characteristic dimension for which the pod width is taken.

$$f[Hz] = \frac{St\,V}{D} = \frac{0.25 \cdot 56.59}{0.4} = 35.37\,Hz$$

$$f[Hz] = \frac{St\,V}{D} = \frac{0.24 \cdot 10.29}{0.4} = 6.17\,Hz$$

The shedding frequency of the pods at a freestream velocity of 110 kts is estimated to be around 35 Hz, while the shedding frequency at a freestream velocity of 20 kts is estimated to be 6.17 Hz. The vortex shedding is expected to induce an oscillating force mainly in x direction and the helicopter structure may then be subject to vibrations. Moreover, the shedding frequencies of the pods, which are close to 6Hz, could for certain flight conditions start to interact with the vibrations caused by the helicopter rotor at a frequency of 1/rev, also in this case rotating at a frequency of 6Hz (6 rotations per second). Despite the fact that the structure is usually detuned from the rotor forcing frequencies at 1/rev, the additional force could induce a stress in the upper fuselage linkages. The ultimate judgement on implications should be addressed to specialists in aircraft structures and stress and fatigue analysts.

4.3 Handling Quality Analysis

The handling qualities of the helicopter have been analysed by looking at various aspects of the stability of the helicopter, using an aft-CG and a weight of 5900kg. The aerodynamic derivatives have been normalized according to the principal inertia moments. The simulations have been performed according to the attitudes provided by the TC HOLDER for the respective speeds (the AOA and AOS are not zero for every flight condition).

The analysis has involved three speeds 80kts, 110kts and 140kts. For each airspeed and each helicopter model (with and without pods) the aerodynamic forces and moments have been extracted from 13 simulations, according to Table 2. The simulations have been performed at SSL with the air density $\rho = 1.225 kg/m^3$.

4.3.1 Static Stability Analysis

Table 6 illustrates the delta of static margins of the baseline helicopter versus the helicopter including HEFS pods, on the longitudinal plane during forward flight for the three above mentioned airspeeds.

For clarity, the main assumptions are repeated:

- Results are generated without using a dynamic simulation tool, so dynamic motions in e.g. pitch and roll attitude are decoupled
- Table 6 shows results when considering the fuselage contribution (from CFD data) and the main rotor (semi-articulated rotor) contribution to the static margins in post-processing of the CFD results

Interpretation:

- The absolute dB_{1s}/dV should be positive: a forward cyclic stick input $(+B_{1s})$ results in an increase in velocity $(+V)$
- The absolute dB_{1s}/dq should be negative: a forward cyclic stick input (+B) results in an increase in 'nose-down' pitch rate (-q)
- A positive Delta (i.e. increase in absolute magnitude) in dB_{1s}/dV means: to reach the same increase in velocity $(+V)$, a larger forward cyclic stick input is needed $(+B_{1s})$, compared to the baseline helicopter. This can be translated to "*more resistance when accelerating*".
- A positive Delta (i.e. increase in absolute magnitude) in dB_{1s}/dq means: to reach the same increase in 'nose-down' pitch rate $(-q)$, a larger forward cyclic stick input is needed $(+B_{1s})$, compared to the baseline helicopter. This can be translated to "*more resistance in pull-up and pull-over manoeuvres*".

The main rotor responds with a delay in the pitch rate manoeuvres and it is subject to a rearward flap while in forward flight. We have considered a semi-articulated rotor and by introducing the term in static margins associated to the Main Rotor, the values become:

Static Margins DELTA Fuselage + Main Rotor Contributions [%]			
	@80kts	**@110kts**	**@140kts**
Longitudinal Static **dB_1/dV**	0.55% (<|1%|)	0.10% (<|1%|)	0.22% (<|1%|)
Longitudinal Static **dB_1/dq**	0.26% (<|1%|)	-1.07%	-1.41%

Table 6 Static Margins variation at 80kts, 110kts and 140kts

From Table 6 for every speed there is a slight positive delta for **dB_1/dV** which means that the installation of the HEFS pods on the CS29 reference helicopter causes slightly more resistance when accelerating. At 80 kts the pods also offer more resistance to pitch rates, while it can also be seen that for 110 kts and 140 kts, the delta for **dB_1/dq** is slightly negative. This means that at high speed due to turbulence in the upper cowling, the HEFS pods cause slightly less resistance in pull-up and pull-over manoeuvres. This may indicate that the presence of the HEFS pods changes the aerodynamics of the entire upper cowling and therefore the overall aerodynamics around the fuselage, even if it is in a small measure.

The increase of the required longitudinal forward cyclic command associated with changed static margins translates in a minimal reduction of the attainable V_D. The ultimate limit of forward cyclic command that can be given as input determines the maximum V_D, therefore the maximum attainable speed can be estimated to be:

$$V_{D,new} = \frac{V_D}{1 + \Delta(\mathbf{dB_1}/\mathbf{dV})}$$

4.3.2 Dynamic Stability Analysis

The fidelity of the simulation model used for this study, has shown to be insufficient for a reliable analysis of the dynamic stability of the CS29 reference helicopter. An assessment has been performed after obtaining the results for the dynamic stability (the delta in period and damping of oscillations of the aircraft by using aerodynamic derivatives, after installation of the HEFS pods) and the following was concluded:

- The magnitude of the uncertainties posed by the model (CFD simulations in combination with necessary assumptions made throughout post-processing of results) outweigh the ‘delta’ to be assessed on the dynamic stability margins.
- The lack of the rotor dynamics does not allow to describe the evolution of the oscillations as well as estimating the positions of poles and zeros of the oscillations’ transfer function.
- The lack in validation data that was available for the study did not make possible to validate the dynamics of the helicopter.

Hence, the results for the dynamic stability analysis remain inconclusive and will be omitted.

4.3.3 Change in Aerodynamic Forces and Moments

The change in aerodynamic derivatives can be explained by a change in aerodynamic forces acting on the aircraft. Table 7 shows the delta between the baseline helicopter and the helicopter including HEFS pods of Forces and Moments acting on the helicopter body only. In some cases, the delta in percentage can appear high, whilst the absolute delta resulting from the CFD simulations is not very high, this has been thoroughly analysed.

Forces & Moments DELTA [%] (fuselage + tail + horizontal stab + pods)							
	Force X	**Force Y**	**Force Z**	**Moment L**	**Moment M**	**Moment N**	**Drag**
80kts	2.6	-8.6	-2.9	-24.7	1.6	-10.7	2.5
110kts	1.5	-6.6	25.0	-20.0	-4.5	-8.6	1.4
140kts	1.7	-5.7	3.5	-17.0	-5.2	-7.5	1.7

Table 7 Delta of Forces and Moments acting on the helicopter body

It is possible to derive the following conclusions:

- The presence of the pods induces the *creation of some rolling moment around the helicopter* $-x$ *axis* due to the presence of the inherent sideslip during forward flight.
- The pods generate *down force along the direction* $+z$ which is prominent at 110kts and then reduces at 140kts.
- There is also a variation of *yawing moment along the direction* $-z$ which can be associated with a loss of efficiency of the vertical fin, given that the wake of the pods might reduce the energy in the flow downstream which may impact the vertical fin.

4.3.4 Loss of effectiveness of Horizontal Tailplane and Vertical Fin

An in-depth analysis on the reason behind the changes in forces and moments revealed slight modifications of the flow properties due to the increased wake of the helicopter as reported in paragraphs 4.2.1 and an almost negligible changing of relative angle of attack to the surfaces. As mentioned in 4.3.3 a loss in effectiveness of the vertical fin can also be deduced in particular flight conditions from a change in yawing moments.

4.4 Mission Performance Analysis

For the mission performance analysis, an aft-CG and the highest take-off weight are assumed (6400kg). The simulations have been performed to obtain data on the drag delta's, at SSL with the air density $\rho = 1.225 kg/m^3$. The analysis has involved three speeds 80kts, 110kts and 140kts. The rpm of the main rotor has been assumed according to the data provided by the TC HOLDER (see 2.1.1).

4.4.1 Drag Delta

One of the effects of the installation of the pods is the increase in drag in forward flight. According to the results obtained from the CFD analysis, presented in Table 8, the increase in drag is lower than the initially predicted 3.8% (at SSL) as obtained in the qualitative analysis (both the qualitative and quantitative drag analyses presented consider the helicopter clean fuselage, excluding contributions of hoist, landing gear). An increase in altitude would result in a decrease in total fuselage drag due to a lower air density, however the delta caused by the HEFS installation in *total fuselage drag* and in *fuselage + rotors drag power* will remain the same according to the model used, as illustrated in Table 9.

TAS [kts]	Fuselage Drag Delta [%]	Fuselage + Rotors Drag Power Delta [%]
80	2.60%	1.26%
110	1.11%	0.55%
140	1.78%	0.90%

Table 8 Delta of Drag force after the installation of HEFS Pods (excluding landing gear and hoist, altitude: SSL)

TAS [kts]	Fuselage Drag Delta [%]	Fuselage + Rotors Drag Power Delta [%]
80	2.60%	1.26%
110	1.11%	0.55%
140	1.78%	0.90%

Table 9 Delta of Drag force after the installation of HEFS Pods (excl. landing gear and hoist, altitude: 5000 ft)

4.4.2 Increase in Power and Fuel consumption

For the performance analysis, the mass of the helicopter has been scaled to match the configuration of aft-CG highest Take-Off Weight of 6400kg (starting from data related to a medium-take-off Weight condition of 5900kg as provided by the TC HOLDER). The aerodynamic effect of the pods has been evaluated considering the increased drag force. This has resulted in an estimation of the necessary increase in rotor Thrust and consequently in Main Rotor and Tail Rotor Torque.

The delta - between the baseline helicopter and the helicopter including the HEFS pods - of power required due to an increase in drag in forward flight is presented in the table below, and ranges between 0.1% and 0.2%. The average delta in fuel consumption can be expected in the same range of figures. The altitude will not influence the delta percentages of the total power required delta, as they only take into account the delta in drag (due to the HEFS pods), and as was seen in Table 9 the drag delta does not change with altitude in the model.

TAS [kts]	Total (Fuselage + Rotors) Power Required Delta [%]
80	0.10%
110	0.09%
140	0.19%

Table 10 Delta of total power required in forward flight (taking into account the fuselage + rotors + hoist + landing gear contributions)

It should be noted that these results can be considered 'optimistic' and may turn out slightly higher in reality due to the following:

- A blockage factor for the Main Rotor was not taken into account. Due to the model used it is not possible to estimate the amount of rotor effectiveness which translates in an increase of rotor Torque and reduced Thrust. This is especially relevant for climb conditions with a high Rate of Climb.
- The chosen design for the pods has been proved to be quite streamlined, however in practice the pod design might be less optimally shaped.

4.4.3 One Engine Inoperative Performance

The aim of the analysis with a One Engine Inoperative condition is to verify that the helicopter is capable of attaining a minimum rate of climb at 80kts, having just one engine running. The assumptions made for this analysis are the following:

- The functioning engine is running at a MCP (max. continuous power) OEI power level. The engine considered is a Pratt & Whitney Canada PT6-67C turboshaft engine and the performance is assumed based on (EASA, EASA Type-Certificate Data Sheet Pratt & Whitney Canada PT6C-67 series engines, 2012) and (AgustaWestland, 2008). The assumptions taken to estimate the degrade in ROC with OEI are validated based on performance graphs from (AgustaWestland, 2008).
- The mass of the helicopter has been scaled to match the configuration of aft-CG highest Take-Off Weight of 6400kg, which affects the Main Rotor and Tail Rotor Torque and Thrust.
- The estimated drag of the Main Rotor Hub, the Hoist and the Landing gear extracted has been included in post processing of the drag computation
- The data comes from simulations of Level Forward Flight conditions, given the fact that for Climb conditions where the Rate Of Climb is usually below 300ft/min, the aerodynamic characteristics of AOA and AOS do not change significantly from Level Forward Flight conditions and therefore the same levels of forces and moments can be expected.
- The effect of altitude is taken into account in the calculations by correcting the drag data calculated by the CFD simulations for altitude (decrease with altitude) and by correcting the engine power available for altitude (decrease with altitude).

The results of the analysis are shown in Table 11, Table 12, Table 13 and Table 14 for different altitudes. The impact of the HEFS on the ROC compared to the base case is linked to the parasitic drag coming from the helicopter body.

TAS [kts]	ROC BASE [ft/min]	ROC HEFS [ft/min]	ROC Decr. [ft/min]	ROC Decr. Ratio [%]
80	761.76	758.81	-2.95	-0.39%
110	110.14	107.01	-3.13	
140	-1488.80	-1498.76	-9.96	

Table 11 Variation of attainable Rate Of Climb in OEI condition, taking into account: fuselage, rotors, hoist, landing gear extracted. Altitude: SSL.

TAS [kts]	ROC BASE [ft/min]	ROC HEFS [ft/min]	ROC Decr. [ft/min]	ROC Decr. Ratio [%]
80	773.70	770.83	-2.87	-0.37 %
110	192.87	189.84	-3.04	
140	-1272.56	-1282.23	-9.67	

Table 12 Variation of attainable Rate Of Climb in OEI condition, taking into account: fuselage, rotors, hoist (landing gear retracted). Altitude: 1000 ft.

TAS [kts]	ROC BASE [ft/min]	ROC HEFS [ft/min]	ROC Decr. [ft/min]	ROC Decr. Ratio [%]
80	737.55	734.87	-2.68	-0.37%
110	204.61	201.77	-2.84	
140	-1161.09	-1170.13	-9.04	

Table 13 Variation of attainable Rate Of Climb in OEI condition, taking into account: fuselage, rotors, hoist (landing gear retracted). Altitude: 3000 ft.

TAS [kts]	ROC BASE [ft/min]	ROC HEFS [ft/min]	ROC Decr. [ft/min]	ROC Decr. Ratio [%]
80	709.37	706.81	-2.55	-0.36%
110	209.84	207.13	-2.70	
140	-1087.00	-1095.61	-8.61	

Table 14 Variation of attainable Rate Of Climb in OEI condition, taking into account: fuselage, rotors, hoist (landing gear retracted). Altitude: 4000 ft.

The relevant result is the one at 80kts. The worst case (at SSL altitude) decrease in Rate of Climb is 2.95 ft/min which correspond to a relative decrease of 0.39% of ROC capability. Although the true degradation in ROC with OEI may be slightly higher due to design inefficiencies and a blockage factor to the main rotor (not taken into account in the tables above), the ROC degradation can still be considered negligible and still ensures the fulfilment of the OEI requirement. For the sake of completeness, the analysis also provides the reduction of ROC for the other speeds which show already a dive tendency for the OEI scenario (in other words, the helicopter is in this case descending due to a lack of power with OEI).

4.5 Engine Inlet Flow Disturbances

In this section, the impact of the pods on the flow quality entering the engine is assessed. Distorted total inlet pressure may cause a loss of the aerodynamic performance of the gas turbine engine. For this particular helicopter, the position of the engine inlet might represent a constraint for the design of the pods. The blunt body placed in front of the engine inlet might introduce flow disturbances such as a pressure loss at the engine inlet vane.
The quality of the engine inlet flow is analysed by looking at the following two factors:

- Total pressure recovery: a higher pressure recovery means better performance of the inlet
- Pressure distortion: less variation in pressure at the engine inlet face means a better performance

As explained in section 1.8 the engine inlet has a mass flow inward of 1.02 [kg/s] and the engine outlet a mass flow outward of 1.02 [kg/s]. The flight conditions which are analysed by means of CFD analysis are presented in Table 15, which are all performed for the model with and without the HEFS pods resulting in 8 CFD simulations. These simulations do not contain any rotor effects, as it can be assumed that at a speed of 110 kts, the downwash of the rotor will not reach the area near the inlet which is analysed in this section.

Variable	Flight condition 1	Flight condition 2	Flight condition 3	Flight condition 4
-	Excl. rotor	Excl. rotor	Excl. rotor	Excl. rotor
Speed	110 kts	110 kts	110 kts	110 kts
Yaw attitude	-10 deg	-5 deg	0 deg	5 deg

Table 15 Flight conditions for engine analysis

It has to be kept in mind that a RANS simulation - which has been conducted - is most suitable for providing mean flow information, and less suitable for providing information about turbulence levels. For this reason, the analysis of the inlet flow disturbances has been performed by looking at total pressure distributions of the mean flow.

4.5.1 Results Total Pressure Recovery

The total pressure recovery at the plane near the engine inlet (local total pressure divided by total freestream pressure) is visualized in 2D heatmaps for each of the simulations, presented in Figure 36. The following observations can be made:

- The pressure recovery of the model with HEFS pods is in general higher and more evenly distributed than the pressure recovery for the base model
- The simulation cases with negative yaw angles have more pressure distortion at the right engine inlet compared to the other cases

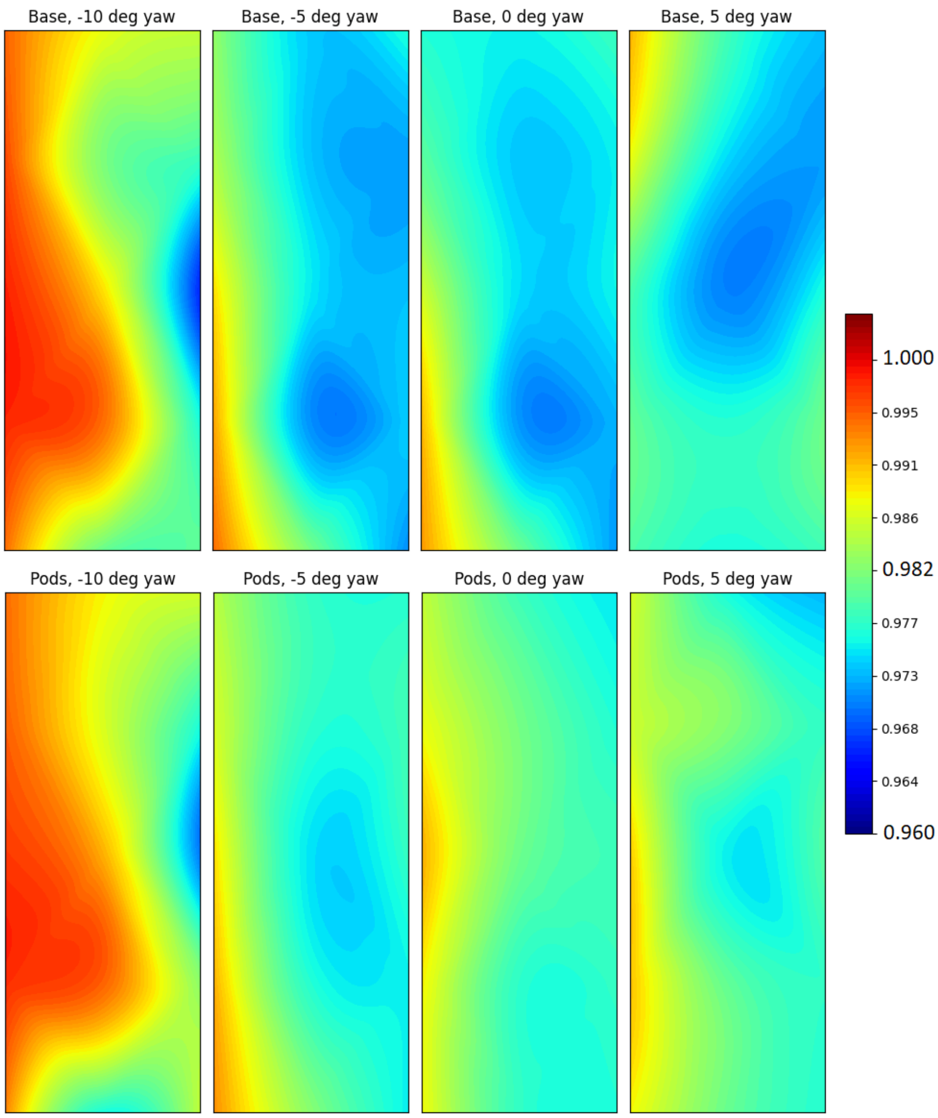

Figure 36 Total pressure recovery near the right engine inlet at 110 kts

In Figure 37 the flow is visualized in a top-view of the base model by means of a SurfaceLIC feature. It can be seen that the recirculation region in the engine inlet is the reason for the total pressure distortions in the heatmap included on the right of the figure. In Figure 38 a zoom-in of Figure 37 is presented.

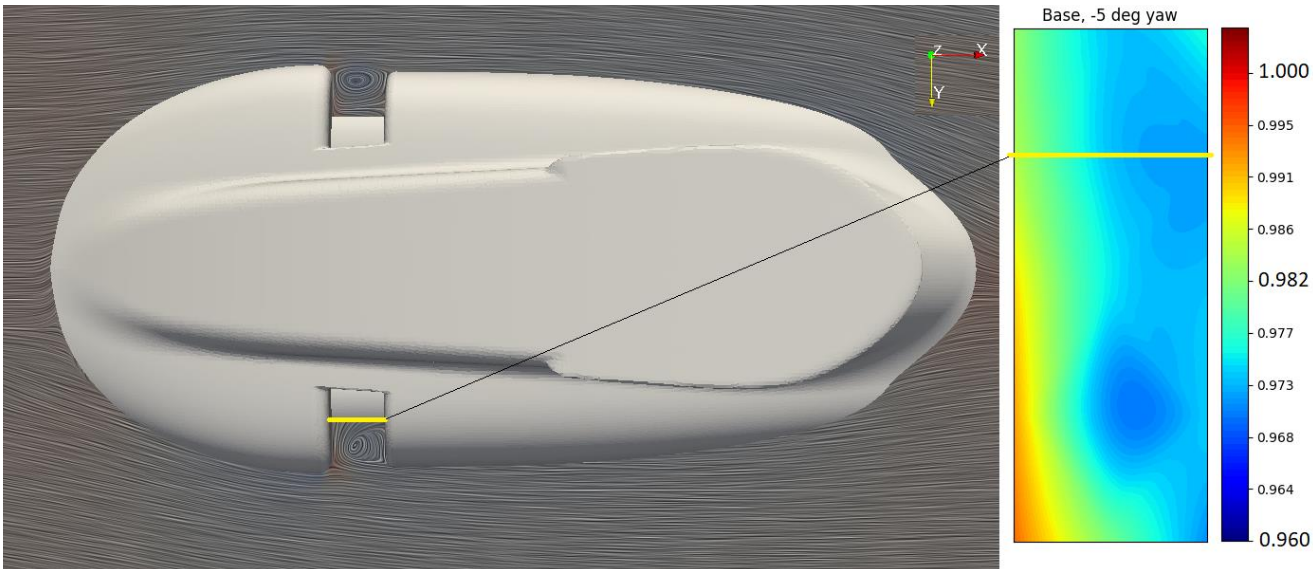

Figure 37 SurfaceLIC topview and pressure recovery of base model at 110 kts

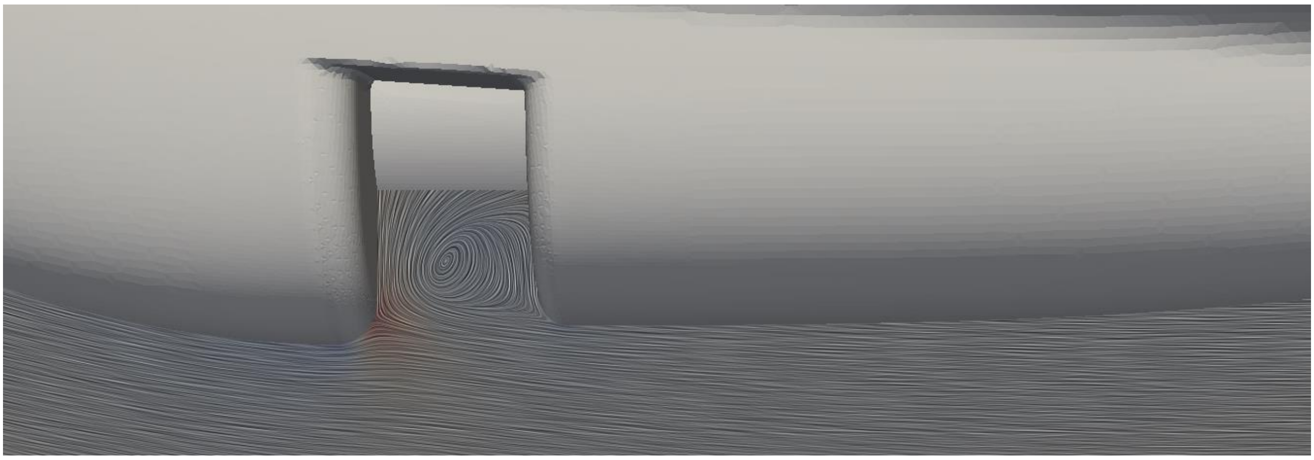

Figure 38 SurfaceLIC topview of base model at 110 kts zoom-in

In Figure 39 the flow is visualized in a top-view of the model including HEFS pods by means of a SurfaceLIC feature. Again it can be seen that the recirculation region in the engine inlet is the reason for the total pressure distortions in the heatmap included on the right of the figure. In Figure 40 a zoom-in of Figure 39 is presented. A very small recirculation area directly behind the pods can be seen, and the recirculation area in the engine inlet is slightly shifted compared to the base model. Apart from that, no major differences in the flow behaviour are observed between the base model and the model with HEFS pods.

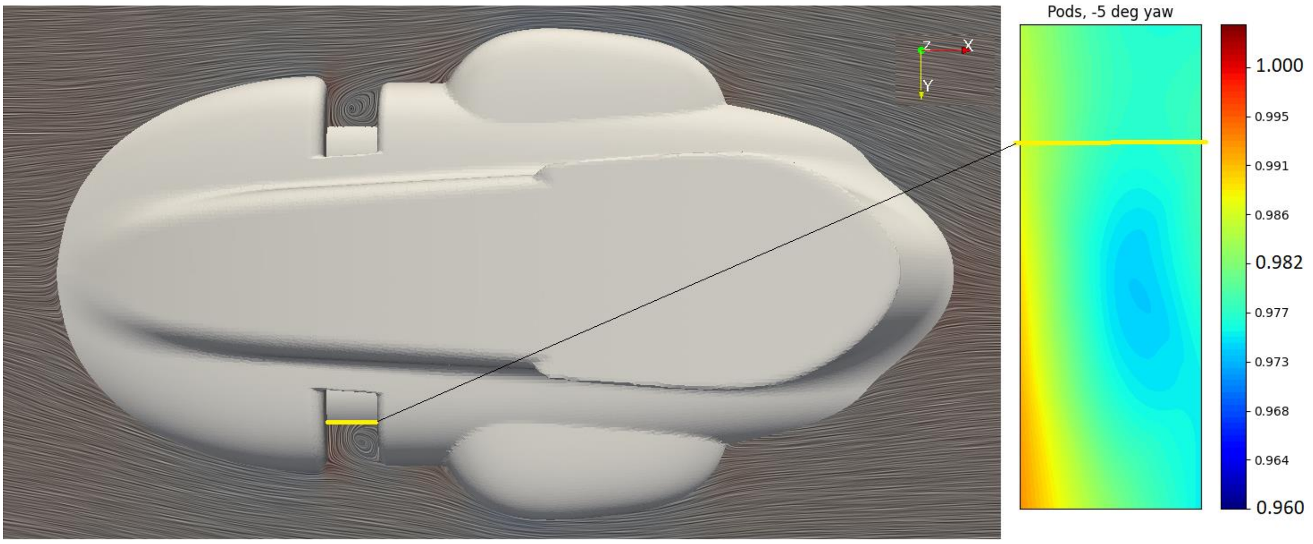

Figure 39 SurfaceLIC topview and pressure recovery of model with HEFS pods at 110 kts

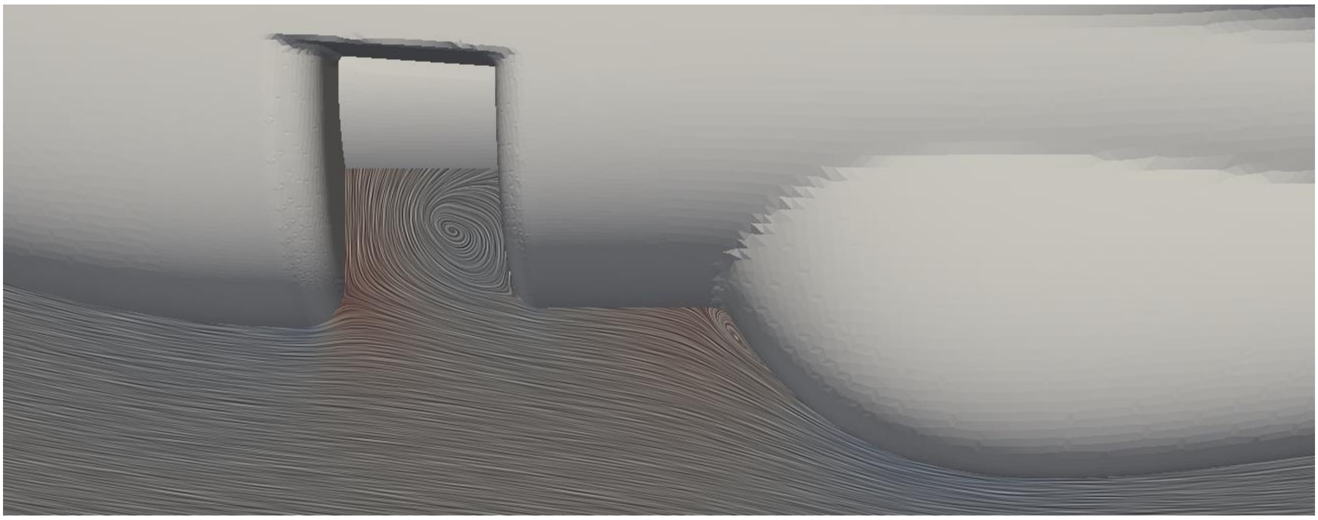

Figure 40 SurfaceLIC topview of model with HEFS pods at 110 kts zoom-in

4.5.2 Results Total Pressure Distortion

The total pressure distortion on the plane near the engine inlet is analysed by looking at the asymmetry both in x- and y-direction and at the outliers. The normalized outliers represent the maximum difference between the measured total pressure in the plane, divided by the average total pressure of the plane. In Table 16 the results from the distortion analysis are presented. The delta analysis indicates that in most cases the asymmetry at the engine inlet plane is lower for the model including the HEFS pods. Also, the normalized outliers are lower for the model including the HEFS pods compared to the base model.

OpenFoam Simulation Case	Asymmetry-x	Asymmetry-y	Outliers
Base, -10 deg yaw	1.94 %	0.14 %	3.20 %
Base, -5 deg yaw	1.55 %	0.39 %	2.39 %
Base, 0 deg yaw	1.07 %	0.40 %	2.12 %
Base, 5 deg yaw	0.75 %	0.15 %	2.11 %
HEFS Pods, -10 deg yaw	1.56 %	0.13 %	2.79 %
HEFS Pods, -5 deg yaw	1.24 %	0.27 %	1.84 %
HEFS Pods, 0 deg yaw	1.14 %	0.06 %	1.66 %
HEFS Pods, 5 deg yaw	1.16 %	0.25 %	1.80 %

Table 16 Distortion analysis total pressure distribution at engine inlet

4.5.3 Conclusions

From the delta analysis performed for the engine inlet flow disturbances, the following is concluded:

- For the different yaw angles, the delta analysis indicates that total pressure recovery near the engine inlet is higher for the model including HEFS pods compared to the base model. This is most likely caused by a different inlet inflow angle as the pods redirect the flow upstream of the engine inlet.
- For most of the simulation cases, the delta analysis shows that the total pressure distribution is more distorted for the base model compared to the model including HEFS pods.
- The RANS simulations show very small recirculation regions behind the pods. Even though RANS in general underestimates recirculation regions, this still gives an indication that it can be expected that the recirculation regions behind the pods are minimal, most likely due to the aerodynamic shape of the design.

Overall, considering the eight simulations performed for the analysis of the engine inflow pressure distribution, the results do not suggest a large impact on the engine inlet flow caused by the HEFS pods. Most likely due to the aerodynamic shape of the pods, the mean flow around the model is redirected in such a way that the total pressure at the engine inlet becomes more uniformly distributed compared to the base model.

5. Quantitative Aerodynamic Assessment CS27

5.1 Wake and Vortex Shedding Analysis

5.1.1 Wake Cross-Sectional Area

A delta analysis (with and without the pod) has been conducted, inspecting the cross-sectional area of the wake behind the helicopter to see what effect the HEFS pods have on the wake propagation for the CS27 Reference Helicopter. For this, a flight speed of 80 kts was evaluated.

In Figure 41, cross-sectional planes (top view) of the CS27 reference helicopter baseline model and the model including HEFS pods are presented, where it can be observed that the outflow of the main gear box exit vane has a strong effect on the wake of the baseline model. The pods redirect the exit flow of the main gear box, which affects the wake shape. In Figure 42 and Figure 43, cross-sectional planes (back view) are presented of the wake. As can be seen from the figures, the wake of the baseline model is slightly bigger than the wake of the model including the pods.

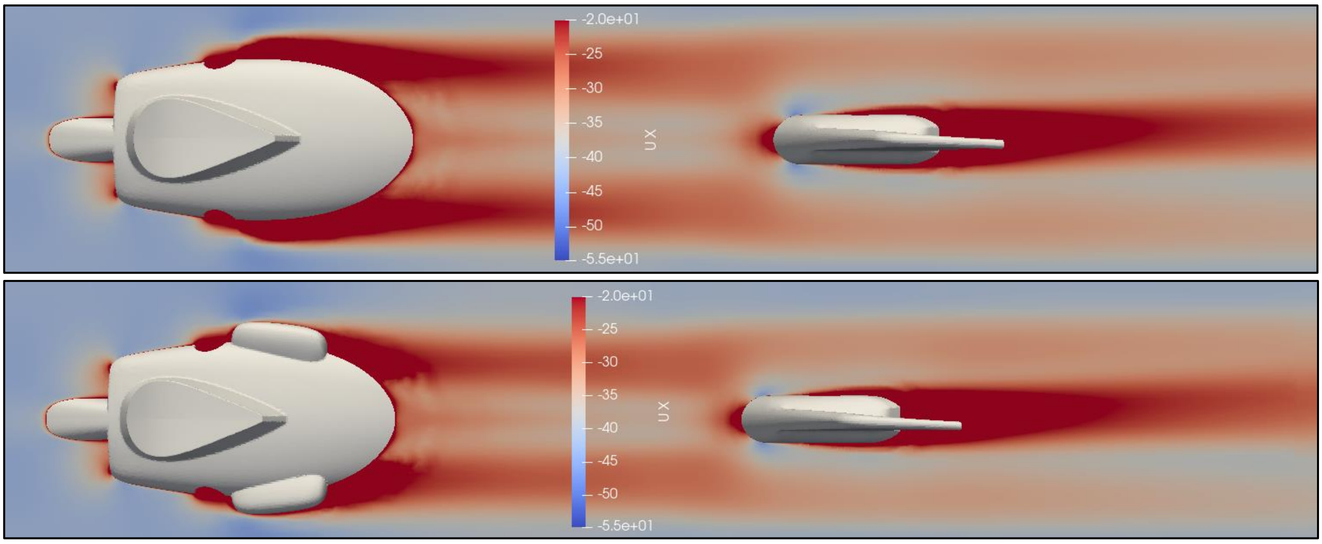

Figure 41 Top View wake propagation CS27 reference helicopter at 80 kts – velocity in x-direction

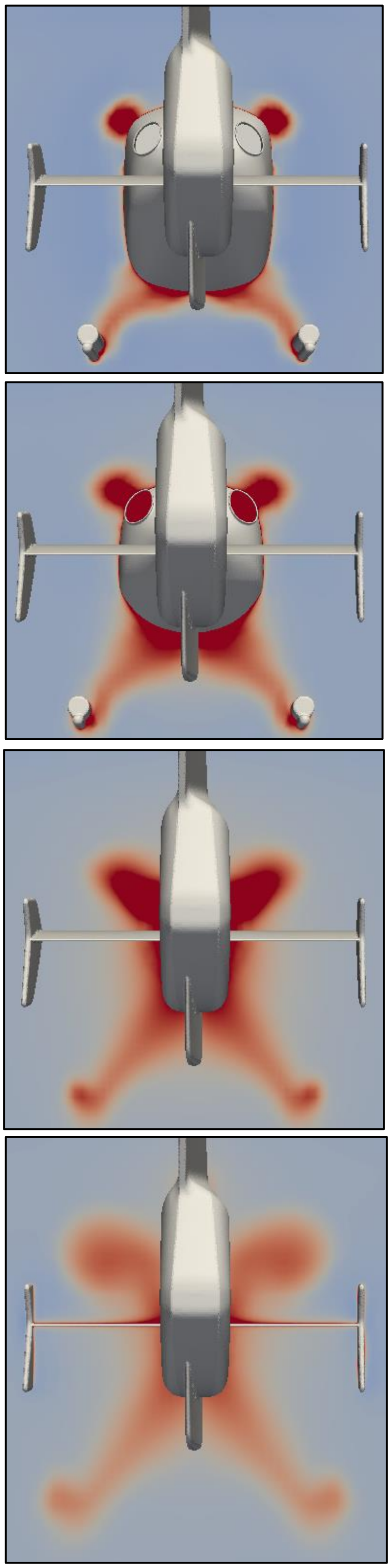

Figure 43 Wake propagation CS27 reference helicopter baseline at 80 kts

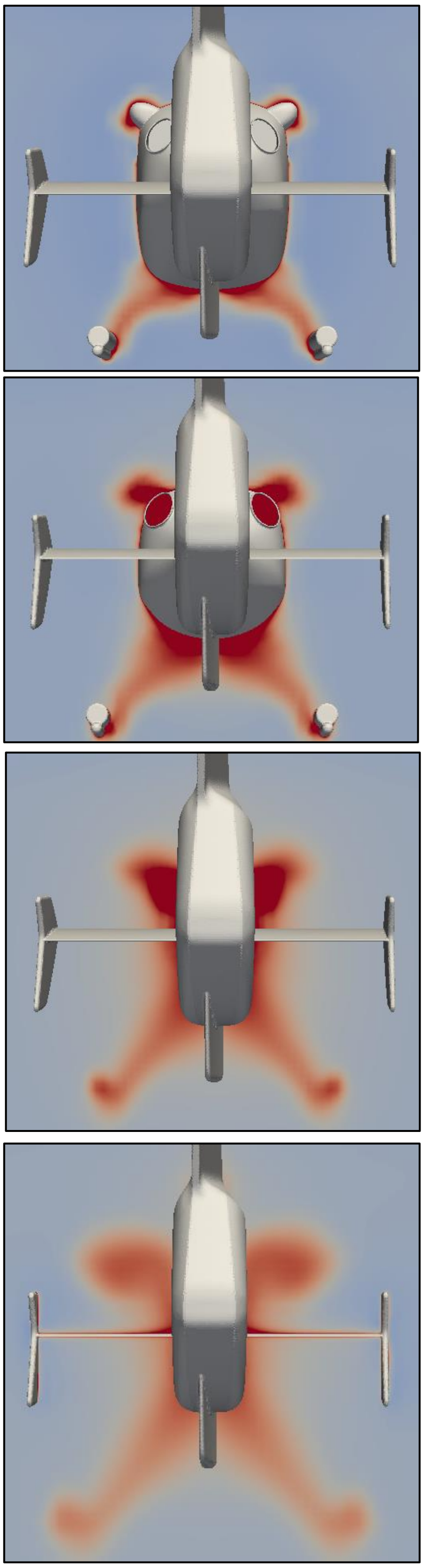

Figure 42 Wake propagation CS27 reference helicopter with pods at 80 kts

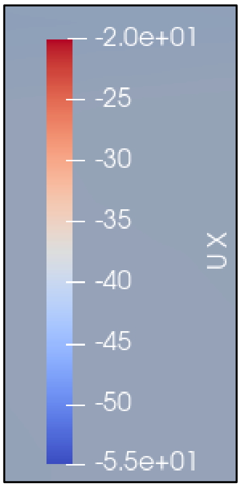

Figure 41, Figure 42 and Figure 43, indicate that the pods do not create an increased wake area. However, it has to be noted that two factors can influence the difference in the wake between the two models: geometric change (HEFS pods) and local grid resolution. In Figure 44 the point cloud of the cell centroids is shown, in a cross-sectional plane seen from a top view. In the baseline model, the flow exiting from the MGB outlet travels through lower grid resolution compared to the MGB outlet flow of the model including HEFS pods, because of the refinement around the pod surface. This causes some uncertainty in the conclusion on the reduced wake area when adding HEFS pods to the geometry.

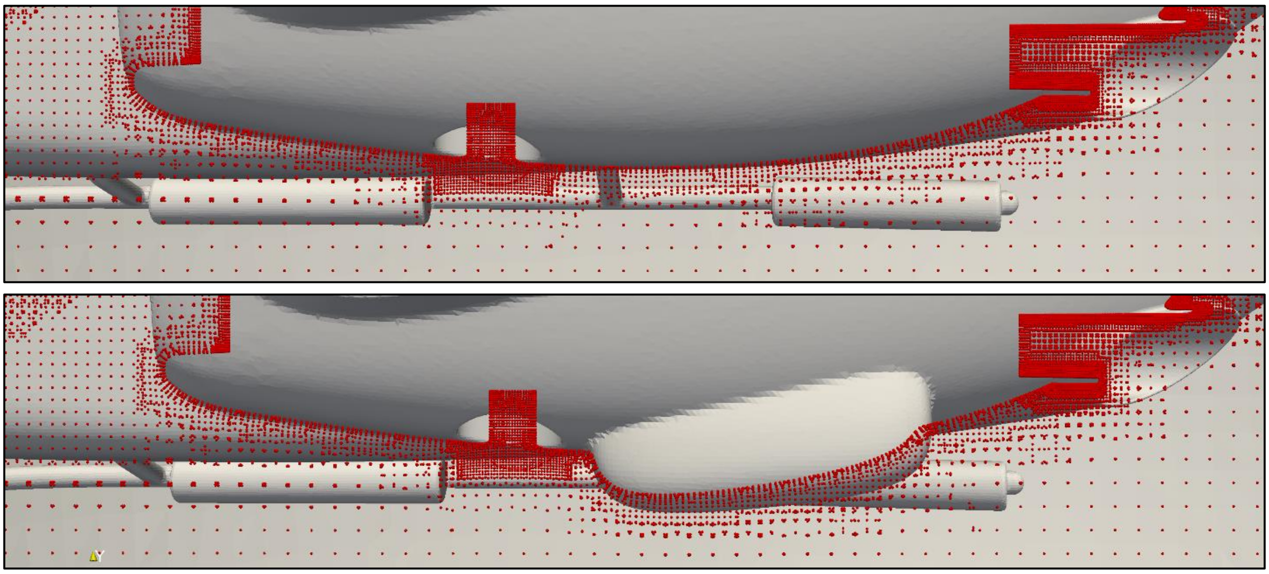

Figure 44 Top view CS27 reference helicopter, point cloud of cell centroids at left side of the helicopter

5.1.2 Vortex Shedding from Pod 2

$$Re_{20kts} = \frac{V\,L}{\nu} = \frac{10.29\ \cdot\ 1.0}{1.5\ \cdot\ 10^{-5}} = 6.86\ \cdot\ 10^{5}$$

The following Strouhal numbers apply to the different flight conditions:

$$St_{110kts} \approx 0.245$$
$$St_{20kts} \approx 0.22$$

The relation for the Strouhal number can then be used to approximate the shedding frequency of vortices from the pods. Here, D is the characteristic dimension for which the pod width is taken.

$$f[Hz] = \frac{St\,V}{D} = \frac{0.245\ \cdot\ 56.59}{0.35} = 39.61\ Hz$$

$$f[Hz] = \frac{St\,V}{D} = \frac{0.22\ \cdot\ 10.29}{0.35} = 6.47\ Hz$$

The shedding frequency of the pods at a freestream velocity of 110 kts is estimated to be around 39.61Hz, while the shedding frequency at a freestream velocity of 20 kts is estimated to be 6.47Hz. The vortex shedding is expected to induce an oscillating force mainly in x direction and the helicopter structure may then be subject to vibrations. The shedding frequencies of the pods, which are close to 6.5Hz, are not expected to interact with the vibrations caused by the helicopter rotor at a frequency of 1/rev, in this case rotating at a frequency of 4.96Hz (4.96 rotations per second) also in the light of the fact that the structure is usually detuned from the rotor forcing frequencies at 1/rev. The ultimate judgement on implications should be addressed to specialists in aircraft structures and stress and fatigue analysts.

5.2 Handling Quality Analysis

Similar to the analysis performed for the CS29 reference helicopter, the handling qualities of the CS27 reference helicopter have been analysed by looking at various aspects of the stability of the helicopter, using an aft-CG and a medium take-off weight of 2600kg. The aerodynamic derivatives have been normalized according to the principal inertia moments. The simulations have been performed according to the attitudes provided by the TC HOLDER for the respective speeds, where the AOA and AOS are not zero for every flight condition. The analysis has involved three speeds 80kts, 110kts and 140kts. For each airspeed and each helicopter model (with and without pods) the aerodynamic forces and moments have been extracted from 13 simulations, according to Table 2. The simulations have been performed at SSL conditions with the air density $\rho = 1.225 kg/m^3$.

5.2.1 Static Stability Analysis

Static Margins DELTA Fuselage + Main Rotor Contributions [%]			
	@80kts	**@110kts**	**@140kts**
Longitudinal Static **dB_1/dV**	-1.1%	-1.3%	-1.8%
Longitudinal Static **dB_1/dq**	2.2%	4.7%	2.7%

Table 17 Static Margins variation at 80kts, 110kts and 140kts

In Table 17 it can be seen that the delta in **dB_1/dV** is negative, which indicates less resistance when accelerating (after installation of the HEFS pods). It is expected that in reality, the delta will be positive where the pods create slightly more resistance. The negative delta's resulting from the simulations and calculations performed for the percentages in Table 17 can be explained along the line of reasoning outlined in 5.2.2 (effect of the MGB outflow on total fuselage drag in the CFD simulations). It can also be seen that the longitudinal static stability $dB1/dq$ is influenced by the HEFS pods, the increase implicates that the HEFS pods create more resistance in pull-up and push-over maneuvers. The magnitude of the effect should be evaluated with dedicated flight test activity. A possible mitigation could be to design more blended pods in the upper cowling of the helicopter.

The increase of the required longitudinal forward cyclic command associated with changed static margins translates in a minimal reduction of the attainable V_D. The ultimate limit of forward cyclic command that can be given as input determines the maximum V_D, therefore the maximum attainable speed can be estimated to be:

$$V_{D,new} = \frac{V_D}{1 + \Delta(\mathbf{dB_1/dV})}$$

5.2.2 Change in Aerodynamic Forces and Moments

The change in aerodynamic derivatives can be explained by a change in aerodynamic forces acting on the aircraft. Table 18 shows the delta between the baseline helicopter and the helicopter including HEFS pods of Forces and Moments acting on the helicopter body only.

Forces & Moments DELTA [%] (fuselage + tail + horizontal stab + skids)							
	Force X	**Force Y**	**Force Z**	**Moment L**	**Moment M**	**Moment N**	**Drag**
80kts	-4.3	2.5	-4.6	1.8	2.9	-0.3	-4.3
110kts	-4.2	0.0	-4.8	2.5	4.6	-0.6	-4.2
140kts	-3.9	1.9	-3.9	3.3	8.3	-0.5	-3.9

Table 18 Delta of Forces and Moments acting on the CS27 helicopter body

In this case it is possible to derive the following conclusions:

- The changes in forces and moments caused by the pods are in general small and are expected to not significantly change the attitude of the helicopter in forward flight.
- The pods slightly lower the force along the direction of +z, which means that this design of pods might cause a slight downlift. The pods' design can however be changed to ensure a neutral lift on a specific flight condition.
- The presence of the pods might cause a reduction in drag of the upper cowling which results in a negative delta values of drag and an increase of pitch down attitude of the fuselage. It could be the case that the pods have a positive effect on the drag, as the MGB outlet ducted vane creates a jet in crossflow for the baseline model. The presence of the pods seems to change the MGB outlet jet5.1.1 (in crossflow) into a flow over a smooth body, which reduces the overall wake of the cowling. However, there is some uncertainty in this reduction of drag related to local cell refinement, as explained in section 5.1.1.

It is of importance to consider the worst case when analysing the effect of the pods on (for example) the helicopter performance, especially when analysing the delta in ROC performance. Therefore, it was decided to assume as a worst-case scenario with the MGB flow deactivated. This causes the pods to create a slight increase in drag, as expected, which can be seen in Table 19.

5.2.3 Loss of effectiveness of Horizontal Tailplane and Vertical Fin

The qualitative analysis of the loss of effectiveness on the tail's aerodynamic surfaces has been performed using the helicopter model with the MGB outflow activated. From Figure 42, it is possible to see how the presence of the pods does not change the airflow energy distribution at the section of the horizontal stabilizer and an almost negligible changing of relative angle of attack to the surfaces. Looking at the wake distribution we can also deduct that the Vertical Fin lies outside of the wake trail, for this reason we do not expect changes in the yawing moment due to the vertical fin.

5.3 Mission Performance Analysis

For the mission performance analysis, an aft-CG and the highest take-off weight are assumed (2800kg). The simulations have been performed to obtain data on the drag delta's, at SSL with the air density $\rho = 1.225 kg/m^3$. The analysis has involved three speeds 80kts, 110kts and 140kts. The rpm of the main rotor has been assumed according to the data provided by the TC HOLDER (see 2.1.1).

5.3.1 Drag Delta

An interesting effect of the installation of the pods that came forward in Table 18 is the reduction in drag, which can most likely be attributed to a more efficient flow introduced by the pods. However, as mentioned in 5.2.2, there is some uncertainty in this conclusion and the worst-case scenario should be considered when analysing the performance. In Table 19 the delta in drag force is presented with the MGB flow in the CFD model deactivated. An increase in altitude would result in a decrease in total fuselage drag due to a lower air density, however the delta caused by the HEFS installation in *total fuselage drag* and in *fuselage + rotors drag power* will remain the same according to the model used, as illustrated in Table 20.

TAS [kts]	Fuselage Drag Delta [%]	Fuselage + Rotor Drag Power Delta [%]
80	1.55 %	1.11 %
110	2.20 %	1.68 %
140	1.79 %	1.41 %

Table 19 Delta in fuselage drag (the body including the tail, horizontal stab and skids, excluding hoist) on the CS27 helicopter, MGB flow deactivated in CFD model. Altitude: SSL

TAS [kts]	Fuselage Drag Delta [%]	Fuselage + Rotor Drag Power Delta [%]
80	1.55 %	1.11 %
110	2.20 %	1.68 %
140	1.79 %	1.41 %

Table 20 Delta in fuselage drag (the body including the tail, horizontal stab and skids, excluding hoist) on the CS27 helicopter, MGB flow deactivated in CFD model. Altitude: 5000 ft.

5.3.2 Increase of Power and Fuel consumption

An important aspect in evaluating the HEFS pods is the capability of the helicopter to fulfil a desired mission and to estimate the power consumption and the fuel consumption.

For performance analysis, the mass of the helicopter has been scaled to match the configuration of aft-CG maximum Take-Off Weight 2800kg (starting from a medium take-off weight condition of 2600kg). The aerodynamic effect of the pods has been evaluated considering the increased drag force. This has resulted in a necessary increase in rotor Thrust and consequently in Main Rotor and Tail Rotor Torque.

The delta - between the baseline helicopter and the helicopter including the HEFS pods - of power required in forward flight ranges between 0.22% and 0.69% and the average delta in fuel consumption per flying hour can be expected in the same range of figures. The altitude will not have an effect on the delta percentages of the total power required delta, as they only take into account the delta in drag (due to the HEFS pods), and as was seen in Table 20 the drag delta does not change with altitude in the model.

TAS [kts]	Total (Fuselage + Rotors) Power Required Variation [%]
80	0.22 %
110	0.60 %
140	0.69 %

Table 21 Delta of total power required in forward flight, taking into account the fuselage (body, tail, horizontal stab, skids and hoist) and rotors

Similar to the CS29 analysis, it is important to note the following:

- With the introduction of a blockage factor for the Main Rotor these estimates might slightly increase. Due to the model used it is not possible to estimate the amount of rotor effectiveness which translates in an increase of rotor Torque and reduced Thrust. This is especially relevant for climb conditions with a high Rate of Climb.
- The chosen design for the pods has been proved to be quite streamlined, although less than the design for the CS29 reference helicopter. It must be kept in mind that the adoption of a pod design which is not so optimally shaped likely slightly increases the power consumption.

5.3.3 One Engine Inoperative Performance

The aim of the analysis with a One Engine Inoperative condition is to verify that the helicopter can attain a minimum rate of climb at 80kts, having just one engine running. The assumptions made for this analysis are the following:

- The functioning engine is running at a MCP (max. continuous power) OEI power level. The engine considered is a Pratt & Whitney PW206B2 turbine engine and the performance is assumed based on (Eurocopter, EC135 Technical Data, 2006). The assumptions taken to estimate the degrade in ROC with

OEI are validated based on performance graphs from (Eurocopter, EC135 Technical Data, 2006) and an NLR article about the qualification of the EC135[1].

- The mass of the helicopter has been scaled to match the configuration of aft-CG maximum Take-Off Weight of 2800kg, which affects the Main Rotor and Tail Rotor Torque and Thrust.
- The estimated drag of the Hoist has been included in post processing in the drag computation. The data comes from simulations of Level Flight conditions, given the fact that for Climb conditions where the Rate Of Climb is usually below 300ft/min, the aerodynamic characteristics of AOA and AOS do not change significantly from Forward Flight conditions and therefore the same levels of Forces and Moments can be expected.
- The effect of altitude is taken into account in the calculations by correcting the drag data calculated by the CFD simulations for altitude (decrease with altitude) and by correcting the engine power available for altitude (decrease with altitude).

The results of the analysis are shown in Table 22, Table 23, Table 24 and Table 25. The impact of the HEFS on the ROC compared to the base case is linked to the parasitic drag coming from the helicopter body.

TAS [kts]	ROC BASE [ft/min]	ROC HEFS [ft/min]	ROC Decr. [ft/min]	ROC Decr. Ratio [%]
80	385.10	379.57	-5.53	-1.46%
110	-475.17	-495.26	-20.09	
140	-1934.22	-1967.08	-32.85	

Table 22 Variation of attainable Rate Of Climb in OEI condition, taking into account: fuselage, rotors, hoist. Altitude: SSL

TAS [kts]	ROC BASE [ft/min]	ROC HEFS [ft/min]	ROC Decr. [ft/min]	ROC Decr. Ratio [%]
80	382.39	377.02	-5.37	-1.42%
110	-446.33	-465.82	-19.50	
140	-1859.83	-1891.72	-31.9	

Table 23 Variation of attainable Rate Of Climb in OEI condition, taking into account: fuselage, rotors, hoist. Altitude: 1000 ft.

TAS [kts]	ROC BASE [ft/min]	ROC HEFS [ft/min]	ROC Decr. [ft/min]	ROC Decr. Ratio [%]
80	370.74	365.72	-5.02	-1.37%
110	-389.81	-408.04	-18.23	
140	-1705.52	-1735.34	-29.82	

Table 24 Variation of attainable Rate Of Climb in OEI condition, taking into account: fuselage, rotors, hoist. Altitude: 3000 ft.

[1] https://dspace-erf.nlr.nl/server/api/core/bitstreams/3fdefe9e-d4e0-499d-acb5-1bb67242ece0/content

TAS [kts]	ROC BASE [ft/min]	ROC HEFS [ft/min]	ROC Decr. [ft/min]	ROC Decr. Ratio [%]
80	357.51	352.73	-4.78	-1.36%
110	-355.51	-372.88	-17.36	
140	-1603.57	-1631.97	-28.40	

Table 25 Variation of attainable Rate Of Climb in OEI condition, taking into account: fuselage, rotors, hoist. Altitude: 5000 ft.

The significant result is the one at 80kts. The decrease in Rate of Climb for the worst case is 5.53 ft/min which correspond to a relative decrease of 1.46% of ROC capability. Although the true degradation in ROC with OEI may be slightly higher due to design inefficiencies and a blockage factor to the main rotor (not taken into account in the tables above), this degradation can be considered negligible and still ensures the fulfilment of the OEI requirement. The analysis also provides the reduction of ROC for the other speeds which show already a dive tendency for the OEI scenario (in other words, the helicopter is in this case descending due to a lack of power with OEI).

6. Conclusion

6.1 Conclusions Reference Helicopters

6.1.1 Objectives

The objective of the aerodynamic study is to determine if the expected aerodynamic impact of the HEFS on CS27 and CS29 certified helicopters will result in unsurmountable degradation in performance and handling qualities. Unsurmountable is defined as impact that causes the helicopter to lose compliance with airworthiness requirements that cannot be mitigated without severe engineering work (e.g. modifying and re-certifying the flight control system), or the aerodynamic impact leads to unacceptable cost penalties for the TC HOLDER or the operators. The approach taken for the aerodynamic impact assessment is a 'delta' analysis, comparing a baseline helicopter with and without the HEFS installed.

6.1.2 CS29 Reference Helicopter and Pod Design

For the CS29 reference helicopter in this project, an aerodynamic pod design has been established based on engineering experience and design 'rules of thumb'. Key geometry constraints have been taken into account, such as mitigation of vortex shedding around the pod, creation of zero net longitudinal forces in hover, mitigating effect on flow quality near the engine inlet, taking into account manufacturing tolerances for the pod, and satisfying the specified location to achieve the defined buoyancy once the floats are deployed.

6.1.3 CS29 Qualitative Aerodynamic Assessment

Based on the first qualitative design assessment, adding the HEFS seems feasible from aerodynamic perspective with acceptable performance (and operational cost) impact and a shape that should minimize flow separation before the engine inlet.

6.1.4 CS29 Quantitative Aerodynamic Assessment

Increased wake cross-sectional area: The HEFS pods induce a slightly upward increased wake area behind the helicopter fuselage. However, the wake disturbances introduced by the engine outlet flow are significantly dominating over the disturbance introduced by the pods.

Vortex Shedding from HEFS pods: The HEFS pods may introduce shed vortices into the flow, which is minimized by a streamlined design of the pod. By looking at the geometric characteristics of the pods and the local Reynolds and Strouhal number, the frequency of vortex shedding has been estimated in a high and low speed flight condition. At 110 kts freestream velocity the shedding frequency is estimated to be in the order of 35 Hz, whereas the shedding frequency at 20 kts freestream velocity is estimated to be in the order of 6 Hz. Structural experts should evaluate any potential problematics which may arise due to these ranges of frequencies.

Handling Quality Analysis – Static Stability: The delta in longitudinal static stability due to the HEFS pods, indicated that the pods cause a slight resistance when accelerating (<1% delta). It was also seen that the HEFS pods cause slightly less resistance in pull-up and pull-over manoeuvres for higher speeds, which may indicate a different kind of behaviour of the entire system due to an impact of the pods to the overall aerodynamics around the fuselage. Since the delta's in longitudinal static stability margins found from the model are relatively small, it is concluded that the impact can be expected to be negligible and possible to mitigate.

Handling Quality Analysis – Dynamic Stability: An assessment of the reliability of the dynamic stability analysis, has shown that the model used for this study is not sufficiently accurate to provide reliable information on the delta in dynamic stability margins. The results for the dynamic stability analysis remain inconclusive.

Handling Quality Analysis – Aerodynamic Forces and Moments: The model indicates that the presence of the pods creates some rolling moment around the helicopter x-axis due to the inherent sideslip during forward flight. Also, the pods generate some down lift which becomes prominent around 110 kts and reduces again at 140 kts flight speed. Also a delta is observed in yawing moment which may indicate a loss of efficiency of the vertical fin caused (in certain flight conditions) by the extended wake induced by the pods and an increased dihedral effect on the helicopter fuselage. It is expected that this effect will not be prominent and can be mitigated by minor changes in the allowed flight envelope or a more optimized pod design.

Mission Performance Analysis – Increase of Drag: The increase in drag due to the presence of the pods – purely considering the effect on a clean fuselage, excluding drag contributions from the rotors, landing gear and possible hoist – resulting from the CFD analysis is in the range of 1.1%-2.6% for flight speeds ranging from 80 kts to 140 kts. These values are lower than the originally estimated increase in drag of 3.8% from the qualitative analysis. Based on the CFD results, the average increase in fuel consumption due to the presence of the pods can be expected in the range of 0.1%-0.2% (taking into account the fuselage, rotors, landing gear extracted and hoist), which in reality may end up slightly higher due to potential inefficiencies in the pod design and the introduction of a blockage factor of the main rotor which was not included in the CFD framework.

Mission Performance Analysis – One Engine Inoperative ROC: The CFD analysis indicates that the presence of the pods causes a degradation in the maximum ROC at 80 kts in the order of 0.39% (equal to a decrease in ROC of 2.95 ft/min). A decrease in ROC of 0.39% (2.95 ft/min) is negligible and will likely not even be measurable in flight tests, hence the fulfilment of the OEI requirement is still ensured and a sufficient margin to avoid hazardous situations is still to be expected (which is deduced amongst others from the quantitative data provided by the TC HOLDER).

Engine Inlet Flow Disturbances: By looking at the total pressure distribution near the engine inlet, the CFD analysis indicates that the presence of the pods does not cause any major pressure losses at the engine inlet compared to the baseline case. In addition to this, the presence of the pods also does not cause any major extra distortions near the engine inlet. It should be noted however that these results are strongly related to the engine inlet location, which is very dependent on the specific helicopter type. The impact on the engine inlet is an area of attention which cannot be generalized for all CS27 and/or CS29 certified helicopters, and thus should be analysed for each specific helicopter type.

6.1.5 CS27 Reference Helicopter and Pod Design

An aerodynamic pod design has been established based on engineering experience and design 'rules of thumb'. In contrast to the CS29 reference helicopter, the CS27 reference helicopter offered a more restricted geometrical design space due to inlet and outlet vanes which should not be covered by the pod. This means that the design of the pod for the CS27 is less optimal from an aerodynamic point of view compared to the design of the CS29 pod. Again, key geometry constraints have been taken into account as far as possible, such as mitigation of vortex shedding around the pod, creation of zero net longitudinal forces in hover, taking into account manufacturing tolerances for the pod, and satisfying the specified location to achieve the defined buoyancy once the floats are deployed.

6.1.6 CS27 Qualitative Aerodynamic Assessment

Based on the first qualitative design assessment, adding the HEFS seems feasible from aerodynamic perspective with acceptable performance (and operational cost) impact. However, due to a quite blunt shape of the pod, more flow separation (and vortex shedding) might occur than was the case for the CS29, which should be evaluated by structural engineers.

6.1.7 CS27 Quantitative Aerodynamic Assessment

Increased wake cross-sectional area: The HEFS pods do not have a large impact on the wake and may even have a slightly positive effect. In other words, the wake cross-sectional area will likely not be significantly increased by the pods, instead it might even be slightly decreased due to a more smooth airflow from the cowling vanes. *Vortex Shedding from HEFS pods:* The HEFS pods may introduce shed vortices into the flow, which is minimized as far as possible by a streamlined design of the pod. By looking at the geometric characteristics of the pods and the local Reynolds and Strouhal number, the frequency of vortex shedding has been estimated in a high and low speed flight condition. At 110 kts freestream velocity the shedding frequency is estimated to be in the order of 40 Hz, whereas the shedding frequency at 20 kts freestream velocity is estimated to be in the order of 6.5 Hz. Structural experts should evaluate any potential structural impacts which may arise due to these ranges of frequencies.

Handling Quality Analysis – Static Stability: The delta in longitudinal static stability suggests that the pods introduce a quite prominent resistance in pull-up and push-over maneuvers (2% - 5% delta). This indicates an area of attention, and the presence and magnitude of this impact should be validated by means of flight test activity. The pods' design should be optimized and should be streamlined and better integrated into the upper cowling, reducing the effect on pitch rate static stability margins. It is also expected that a slight resistance will be introduced when accelerating, it is advised to validate the magnitude of this impact in flight tests.

Handling Quality Analysis – Dynamic Stability: An assessment of the reliability of the dynamic stability analysis, has shown that the model used for this study is not sufficiently accurate to provide reliable information on the delta in dynamic stability margins. The results for the dynamic stability analysis remain inconclusive.

Handling Quality Analysis – Aerodynamic Forces and Moments: The changes in forces and moments due to the pods indicated by the model are in general small and are expected to not significantly change the attitude of the helicopter in forward flight. This design of pods might cause a slight uplift due to the blunt shape of the pods which protrude from the upper cowling. The pods' design should be optimized to ensure a neutral lift on a specific flight condition.

Mission Performance Analysis – Increase of Drag: In the worst-case scenario, the increase in drag due to the presence of the pods – purely considering the effect on a clean fuselage including the skids, excluding drag contributions from the rotors and possible hoist - can be expected to be in the range of 1.55% - 2.20%. Based on the increase in fuselage drag, the increase in fuel consumption can be estimated in the range of 0.22%-0.69% (taking into account the fuselage, rotors, skids and hoist). It can be expected that this increase in fuel consumption in reality may be slightly higher due to potential inefficiencies in the pod design and the introduction of a blockage factor of the main rotor which was not included in the CFD framework.

Mission Performance Analysis – One Engine Inoperative ROC: The CFD analysis indicates that the presence of the pods causes a degradation in the maximum ROC at 80 kts in the order of 1.46% (equal to a decrease in ROC of ~5.53 ft/min). This degradation is considered to be negligible and will likely not even be measurable in flight tests, hence the fulfilment of the OEI requirement is still ensured and a sufficient margin to avoid hazardous situations is still to be expected.

6.2 Generalized Conclusions CS29 and CS27 Cat A Fleet

To provide a definitive and fully argued position on whether the provision of the required high-level flotation units is likely to create disproportionate aerodynamic challenges to helicopter designers, the results of the study must be applied and referred to a generic CS29 and CS27 helicopter where possible.

It should be noted that this study is based on two very clean 3D models of the reference helicopters, for the purpose of using them in the CFD software environment. In reality, the reference helicopters will have significantly more irregularities in for example the fuselage surface. This results in *conservative* delta's, since the delta caused by the pods as found in this study will be referred to the 'very clean' reference helicopters.

The two helicopters analyzed present different aerodynamic efficiency and different mission flight profiles and geometrical design space for retrofitted HEFS pods. The aerodynamic behavior as highlighted in the analysis showed some common characteristics, which allows to extend and generalize some of the results to a variety of helicopters. Some of the results are expected to be specific per helicopter and are advised to be evaluated case by case.

Different attributes play a role in affecting the aerodynamic impact of the HEFS pods:

- *Fuselage Aerodynamic Efficiency*: Streamlined body (AW139) or Blunt body (EC135)
- *Speed*: High-Speed Cruise or Low-Speed Cruise
- *Pod Design Space*: The physical design space available affects the efficiency of the shape of the pod

It has been shown in the study that altitude does not have a large impact on the trend analysis. Furthermore,it can be reasoned that the pods are blunt bodies positioned onto the upper cowling, positioned rearward and above the helicopter CG, therefor the lever arms with respect to the helicopter's body x axis and z axis create a pitch up attitude, an increased dihedral effect of the fuselage and offer resistance in pitch rates, irrespective of the helicopter configuration or flight condition. The design of be pods must be carried out by ensuring the equilibrium of forces in hover, while optimizing the performance in forward flight or quarter flights.

6.2.1 Increased Wake Cross-Sectional Area

The HEFS pods are blunt bodies installed in the upper cowling, located in the section of the fuselage structure affected by a static pressure recovery. This is a critical area since recirculating phenomena might occur due to gradients of pressure, determining the size of the Wake Cross-Sectional area of the helicopter upper fuselage. The helicopters with aerodynamic efficient fuselages (generally CS29 certified helicopters) see an increase of cross-sectional wake due to the pods. In more blunt fuselage designs (generally CS27 certified helicopters) the presence of the pods does not induce a significant increase of the cross-sectional wake. An increase in cross-sectional wake will introduce and increase in the pressure drag of the aircraft and may introduce a reduction in the effectiveness of the horizontal stabilizers and the vertical fin. From the analysis, it was shown that this will most likely be a negligible impact.

6.2.2 Vortex Shedding from HEFS pods

Irrespective of the helicopter type the vortex shedding might induce vibrations on the fuselage which should be evaluated from a structural point of view. The CS27 certified helicopters are in general expected to be forced to have a more blunt HEFS pod design due to restricted design space, resulting potentially in more evident vortex shedding compared to CS29 certified helicopters.

6.2.3 Handling Qualities

The delta's in longitudinal static stability margins indicate that (especially for a blunt HEFS pod design) it can be expected that the pods will cause a quite noticeable resistance (i.e. requires larger control forces) in pull-up and push-over manoeuvres at high speeds which may affect the handling quality (up to 5% delta in key stability derivatives). It can also be expected that a slight resistance will be introduced when accelerating (up to 2% delta), although less prominent than the resistance in pull-up and push-over manoeuvres. Taking into account the limitations of the simulation model it is advised to validate the magnitude of these impacts in flight tests.

6.2.4 Mission Performance

It was shown that the degradation in ROC performance with OEI can be expected to be negligible for the reference helicopters. When considering the CS29 and CS27 certified helicopters in general, it may depend on the specific helicopter whether the degradation is acceptable. However, it can be expected that for the majority of the cases the impact is negligible since it was shown that the order of magnitude of the degradation ranges between 3 - 6 ft/min.

6.2.5 Engine Inlet Flow Disturbances

With an aerodynamic design of the HEFS pod – such as the design for the CS29 reference helicopter in this study – the HEFS pod will create a minimal recirculation region and slightly redirect the flow around the upper cowling. Even with an engine inlet placed directly aft of the streamlined pod, it is unlikely that any problems will arise related to the pressure recovery at the engine inlet. A potential criticality may arise for bluntly designed HEFS pods (due to e.g. physical design restrictions) which have an engine inlet placed directly aft of the pod. In those situations it is advised to evaluate the impact case by case.

6.3 Summarized Conclusions using KPI's

A high level overview is presented of the generalized results, in the form of a test against the identified KPI's. In Table 26, for each KPI, the results from the worst case scenario - from the range of scenario's which were analysed- is tested and presented. By means of this test, it will be clear which aspects of the aerodynamic impact of the HEFS pods are expected to be negligible, and which aspects are indicated by the study to be an area of attention. The aspects indicated as area of attention are advised to be further validated and methods of mitigation should be explored when implementing the HEFS. The key performance indicators (KPI's) identified for this study are the following: pressure recovery at engine inlet plane, delta in static stability margin, reduction in the rate of climb with OEI, increase in fuel consumption. If the KPI falls within the following ranges, it is considered to be a negligible impact[2]:

1. A reduction in pressure recovery at the engine inlet: < 5% (at the worst case scenario[3])
2. A delta in static stability margin of maximum ±10%
3. A reduction in the rate of climb with OEI[4]:
    a. CS29: < 5% (i.e. in the order of 10ft/min)
    b. CS27: < 5% (i.e. in the order of 10ft/min)

---

[2] The KPI's are based on the certification specifications, data provided by the TC HOLDER's and expert engineering judgement

[3] The worst case scenario in this case is defined as the scenario (from the set of analysed cases) where the largest difference in pressure recovery is found at a specific location in the analysed plane.

[4] The KPI is based on expert engineering judgement. It should be noted that the acceptable reduction in *ROC with OEI* depends strongly on margin the specific helicopter in question (without retrofitted pod) already has with the *ROC with OEI* requirement.

4. An increase in fuel consumption[5]: < 2 %

KPI	Negligible Impact / Area of Attention		Comments
	CS29 Generalized	CS27 Generalized	
1. Engine inlet pressure recovery	Negligible Impact	Negligible Impact (Case by Case)	The results indicate that the HEFS pods will most likely not create any problems related to the engine inlet pressure recovery, even when placed close to the engine inlet vane. However, for a blunt pod closely placed before an inlet vane, it is advised to assess case by case.
2. Static stability margin	Negligible Impact	Area of Attention	The results indicate that the increased resistance in pull-up and push-over manoeuvres for the CS27 due to the pods might be quite prominent. The worst-case delta was still below 5%, however the longitudinal static stability for CS27 helicopter is highlighted as an area of attention and the magnitude of the impact should be evaluated in flight tests. The impact on CS29 helicopters is expected to be acceptable, especially after mitigation methods. Potential mitigation can be achieved by optimizing the pods design (more streamlined) and/or more blended pods into the helicopter upper cowling.
3. ROC OEI	Negligible Impact	Negligible Impact	For both CS29 and CS27 reference helicopter the degradation in ROC with OEI is negligible, the order of magnitude of the degradation in ROC with OEI is found to be so small, that it can be expected not to pose any challenges for CS27 and CS29 certified helicopters in general. Potential mitigation can be achieved by more streamlined and/or more blended pods into the helicopter upper cowling.
4. Fuel consumpt ion	Negligible Impact	Negligible Impact	The increase in fuel consumption (due to added drag caused by the HEFS pods) for both classes of helicopters is below 1%, which is deemed a negligible impact. It must be noted that this approximation is somewhat optimistic, in reality it may be slightly higher due to necessary trade-offs in the design.

Table 26 Aerodynamic Impact Assessment of retrofitted HEFS pods on Generalized CS29 and CS27 helicopters

[5] The acceptable increase in fuel consumption strongly depends on the business case of the operator in question, for the sake of the generalized analysis it is assumed that an increase of 2% in fuel consumption can be considered acceptable.

6.4 Final Recommendation to EASA

The expected outcome of the aerodynamic assessment study was to provide a fully argued position on whether the provision of the required high-level flotation units is likely to create disproportionate aerodynamic challenges to helicopter designers. 'Disproportionate aerodynamic challenges' was translated to 'unsurmountable degradation in performance and handling qualities'.

The following definition of unsurmountable is used:

- The aerodynamic impact of installing the High EFS compromises the helicopter airworthiness, operational safety which cannot be 'repaired' or mitigated with reasonable measures. This includes in particular potential non-compliance to the performance and handling qualities requirements of CS27 and CS29 type certificate requirements.
- The aerodynamic impact leads to unacceptable cost penalties for the TC HOLDER: in terms of (aerodynamic) certification (flight test, wind tunnel tests).
- The aerodynamic impact leads to unacceptable cost penalties for the helicopter operators: in terms of operational costs (fuel burn, loss of payload or range due to drag penalty) which have a detrimental effect on the mission capability of the helicopter.

Based on the aerodynamic assessment, it can be stated that it is not likely that the HEFS units will create disproportionate aerodynamic challenges to helicopter designers, that cannot be mitigated. Based on the results obtained in the study, a positive position can be taken toward retrofitting of HEFS pods for CS27 and CS29 helicopters, under the following conditions:

1. The areas of attention identified in the study are validated in flight tests:
   The impact of the HEFS pods on static (and dynamic stability) is identified as an area of attention (especially for CS27 helicopters, where it is expected that the pod design is forced to be more blunt due to restricted geometrical design space). The impact is not expected to be unsurmountable, but the presence and magnitude should be validated in flight tests, where in some cases also a validation of the autopilot may be required.

   Another area of attention is vortex shedding, which is a phenomena which is likely to occur from installations such as the HEFS pods, especially for blunt designs. It is advised that the occurrence and severity of the phenomena is validated in flight tests and structural engineers judge the effect on the helicopter structure. The impact is not likely to pose unsurmountable challenges, but should receive attention when designing and retrofitting the HEFS.

2. Case by case evaluation is recommended in some identified cases:
   Although in most cases the HEFS pod is not expected to negatively affect the quality of the inflow into the engine inlet, in some cases it should be evaluated. These cases involve specific helicopters which will be forced to have a blunt pod shape due to geometrical design restrictions and will have an engine inlet placed downstream and close to the HEFS pods.

3. Proposed methods of mitigation are applied:
   Optimization of pods design: From aerodynamic perspective, it is of importance that the design of the HEFS pod is optimized to minimize the aerodynamic impact. When retrofitting the HEFS, it is advised to optimize the shape and location of the HEFS pods case-by-case.
   HEFS pods blended into helicopter design: It is expected that in the case of directly implementing the HEFS into the helicopter design, instead of retrofitting, the aerodynamic impact will be minimal. All aerodynamic effects caused by the retrofitted HEFS pods, can be largely mitigated by integrating the

system directly into a (new) helicopter design. This can be attributed to the fact that, e.g., autopilot settings and vent/inlet locations and designs will be directly taking the presence of HEFS into account.

7. Bibliography

A. Cooke, E. Fitzpatrick. (2002). *Helicopter Test and Evaluation.*

AgustaWestland. (2008). *AW139 Rotorcraft Flight Manual.*

Antoniadis, A., Drikakis, D., Zhong, B., Barakos, G., Steijl, R., Biava, M., . . . Khier, W. (2012). Assessment of CFD methods against experimental flow measurements for helicopter flows. *Aerospace Science and Technology*(Elsevier).

Arra, M. (2001). *L'elicottero.* Hoepli.

David Reich, R. S. (2016). A Review of 60 Years of Rotor Hub Drag andWake Physics: 1954–2014. *JOURNAL OF THE AMERICAN HELICOPTER SOCIETY 61*.

EASA. (2012). *EASA Type-Certificate Data Sheet Pratt & Whitney Canada PT6C-67 series engines.*

EASA. (2016). *Notice of Proposed Amendment 2016-01 Helicopter ditching and water impact occupant survivability.*

EASA. (2021). *Type Certificate Data Sheet for AW139.*

EASA. (2022). *Type Certificate Data Sheet for EC135.*

Eurocopter. (2006). *EC135 Technical Data.*

Eurocopter, & Aerazur. (2007). Study on Helicopter Ditching and Crashworthiness, EASA.2007.C16.

Flores, A., Takahashi, R., & Mutter, Z. (2021). *D2 Reference Helicopter Report (DAET-2).*

Huot, R. (2013). *Improving the modeling of the Fenestron in the Eurocopter.* Marignane, France.

M. Fuchs, F. Le Chuiton, C. Mockett, J. Sesterhenn and F. Thiele. (2015). Detached-Eddy Simulation of SeparatedWake Flow Around Complex HelicopterFuselage Configuration. (Springer).

Mockett, C. (2012). Helicopter Fuselage Wake Prediction UsingDetached-Eddy Simulation. (Springer).

Shur, M., Spalart, P., Strelets, M., & Travin, A. (2011). A rapid and accurate switch from RANS to LES in boundary layers using an overlap region. *Flow, Turbulence and Combustion*.

U.S. Naval Test Pilot School. (1995). *USNTPS-FTM-No. 107, Flight Test Manual - Rotary Wing Stability and Control.*

U.S. Naval Test Pilot School. (1996). *USNTPS-FTM-No. 106, Flight Test Manual – Rotary Wing Performance.* Maryland.

Wahono, S. (2013). Development of Virtual Blade Model for Modelling Helicopter Rotor Downwash in OpenFOAM. (Aerospace Division Defence Science and Technology Organisation).

European Union Aviation Safety Agency

European Union Aviation Safety Agency

Konrad-Adenauer-Ufer 3
50668 Cologne
Germany

Mail EASA.research@easa.europa.eu
Web www.easa.europa.eu

An Agency of the European Union